Research Square

Preprints are preliminary reports that have not undergone peer review.
They should not be considered conclusive, used to inform clinical practice,
or referenced by the media as validated information.

Psilocybin induces delayed and dynamic changes in human sleep neurophysiology: Results from a randomized controlled trial of psilocybin assisted therapy in patients with comorbid major depressive and alcohol use disorder

Matthew J. Reid

mreid27@jhmi.edu

Johns Hopkins University

Eli Weissman

Johns Hopkins University

Luis Luna Martinez

Johns Hopkins University

Zarmeen Zahid

Johns Hopkins University

Caitlin M. DuPont

Johns Hopkins University

Hongmin Dai

Johns Hopkins University

Patrick H. Finan

University of Virginia

Frederick S. Barrett

Johns Hopkins University

Research Article

Keywords: Psilocybin, Psychedelics, Sleep Electroencephalography (EEG), Sleep Neurophysiology, Slow-Wave Activity, Sleep Oscillations, REM Sleep, Neuroplasticity, Major Depressive Disorder, Alcohol Use Disorder

Posted Date: November 17th, 2026

DOI: https://doi.org/10.21203/rs.3.rs-11333812/v1

License: This work is licensed under a Creative Commons Attribution 4.0 International License.
Read Full License

Additional Declarations: Competing interest reported. MJR is the patent holder for a wireless sleep-EEG system with intended use in precision medicine applications. FSB is a scientific advisor for and holds stock in MindState Design Labs, LLC, and is a scientific advisor for Mind Pharmaceuticals.

Psilocybin induces delayed and dynamic changes in human sleep neurophysiology: Results from a randomized controlled trial of psilocybin assisted therapy in patients with comorbid major depressive and alcohol use disorder.

*Matthew J. Reid[1,2,3], Eli Weisman[1,2]., Luis Luna Martinez[1,2]., Zarmeen Zahid[1,2]., Caitlin M. DuPont [1], Hongmin Dai[1]., Patrick H. Finan [4,1]., Frederick S. Barrett [1,2,5,6]

[1] Johns Hopkins University, Department of Psychiatry and Behavioral Sciences. 5510 Nathan Shock Drive, Baltimore, MD, USA, 21224

[2] Center for Psychedelics and Consciousness Research, Department of Psychiatry and Behavioral Sciences, Johns Hopkins University School of Medicine, 5510 Nathan Shock Drive, Baltimore, MD, USA, 21224

[3] Johns Hopkins Bloomberg School of Public Health, Department of Mental Health, 615 North Wolfe Street Baltimore, MD, USA, 21205

[4] University of Virginia, Department of Anesthesiology, 1215 Lee Street P.O. Box 800710, Charlottesville, VA , USA, 22908

[5] Department of Neuroscience, Johns Hopkins University School of Medicine, 725 North Wolfe Street, Baltimore, MD, USA, 21205

[6] Department of Psychological and Brain Sciences, Johns Hopkins University, Ames Hall, 3400 North Charles Street Baltimore, MD, USA 21218-2686

Corresponding author: Matthew J Reid* BMedSci MSc DPhil: (mreid27@jhmi.edu) Suite 100, 5510 Nathan Shock Drive, Department of Psychiatry and Behavioral Sciences, Johns Hopkins University School of Medicine, Baltimore MD, USA. 21224

Conflicts of Interest: MJR is the patent holder for a wireless sleep-EEG system with intended use in precision medicine applications. FSB is a scientific advisor for and holds stock in MindState Design Labs, LLC, and is a scientific advisor for Mind Pharmaceuticals.

Funding: This study was funded through extramural support from The Sleep Research Society, The Steven & Alexandra Cohen Foundation, and intramural funding from Johns Hopkins School of Medicine.

Contributions: M.J.R.: Conceptualization, Formal analysis, Investigation, Visualization, Writing – original draft, Writing – review & editing, Funding acquisition. E.W.: Investigation, Writing – review & editing. L.L.M.: Investigation, Visualization, Writing – review & editing. Z.Z.: Formal analysis, Investigation, Writing – review & editing. C.M.D.: Conceptualization, Formal analysis, Writing – review & editing. H.D.: Formal analysis, Visualization, Writing – review & editing. P.H.F.: Conceptualization, Supervision, Funding acquisition, Writing – review & editing. F.S.B.: Conceptualization, Investigation, Funding acquisition, Writing – review & editing. All authors reviewed and approved the final manuscript and agree to be accountable for the work.

Abstract:

Rationale: Psilocybin has demonstrated therapeutic potential for major depressive disorder (MDD) and alcohol use disorder (AUD). However, its effects on sleep neurophysiology, particularly beyond the acute pharmacological period, remain poorly understood.

Objectives: To characterise the acute and post-acute temporal dynamics of sleep neurophysiology following psilocybin-assisted therapy in individuals with comorbid MDD and AUD.

Methods: In a randomised, placebo-controlled trial, 40 participants (psilocybin: n = 22; placebo: n = 18) underwent home-based sleep electroencephalographic (EEG) monitoring for three nights preceding and seven nights following administration. Longitudinal changes in spectral activity, sleep architecture, and sleep continuity were examined using nonlinear mixed-effects models.

Results: Significant treatment-by-night interactions revealed delayed, nonlinear alterations in sleep neurophysiology following psilocybin administration, with limited acute effects. NREM slow-wave activity (SWA), NREM sigma, REM sigma, and REM beta exhibited distinct curvilinear trajectories, reaching local minima (SWA) or maxima (sigma and beta) approximately 3–4 nights after administration. Sleep efficiency and total sleep time increased during the first three post-treatment nights, whereas sleep architecture, REM density, sleep onset latency, and delta sleep ratio remained largely unchanged. On the first post-treatment night, increased sleep efficiency was the only observed change, with no significant spectral or architectural alterations.

Conclusions: Psilocybin-assisted therapy induces delayed, dynamic alterations in human sleep neurophysiology extending beyond the acute pharmacological period. These findings suggest that sleep EEG may provide a sensitive measure of evolving neurophysiological processes following psilocybin administration.

Keywords:

Psilocybin; Psychedelics; Sleep Electroencephalography (EEG); Sleep Neurophysiology; Slow-Wave Activity; Sleep Oscillations; REM Sleep; Neuroplasticity; Major Depressive Disorder; Alcohol Use Disorder.

Introduction

Major Depressive Disorder (MDD) is the second leading cause of disability worldwide and the most common psychiatric disorder associated with suicide (Goldberg et al., 2020). Nearly one-third of patients with MDD also present with alcohol use disorder (AUD) (Panin & Peana, 2019) which exacerbates depressive symptoms and further increases risk of suicidal behavior (Conner et al., 2014). A common (36-92% complaint spanning both these disorders is chronic sleep disturbance and insomnia (Chakravorty, Chaudhary et al. 2016, Geoffroy, Hoertel et al. 2018), which also serves to perpetuate drinking behaviors in AUD (Chakravorty, Chaudhary et al. 2016). Particularly in AUD, these sleep disturbances often fail to resolve following recovery, only declining in prevalence to 50% following four weeks of sobriety (Brower, Aldrich et al. 2001, Kolla, Schneekloth et al. 2014, Chaudhary, Kampman et al. 2015, Miller, Donahue et al. 2017). Sleep disturbances not only reduce the effectiveness of interventions for both MDD and AUD (Stein and Friedmann 2006, Troxel, Kupfer et al. 2011, Manglick, Rajaratnam et al. 2013, Edinger, Manber et al. 2017, Koob and Colrain 2020, Lechinger, Koch et al. 2021), but also increase the likelihood of relapses of both disorders (Arnedt, Conroy et al. 2007, Troxel, Kupfer et al. 2011, Chakravorty, Chaudhary et al. 2016, Inada, Enomoto et al. 2021).

Administration of the classic (5HT2A partial agonist) psychedelic psilocybin, in combination with psychological support (Psilocybin-Assisted Therapy, or 'PAT'), offers notable promise for symptom reduction for both MDD (Goldberg, Pace et al. 2020, Carhart-Harris, Giribaldi et al. 2021, Davis, Barrett et al. 2021, Hosein, Reid et al. 2025) and AUD (Bogenschutz, Ross et al. 2022, Jensen, Stenbæk et al. 2025) , and may offer promise in patients with co-occurring disorders. Our prior data (Reid, Kettner et al. 2024) indicates that a single administration of psilocybin significantly improves subjective reports of sleep quality for up to one month in a community sample of individuals attending psilocybin-retreats. However, to our knowledge, no study has explored the impact of PAT on sleep neurophysiology measured objectively using sleep-EEG in a clinical population.

Sleep disturbance in both MDD and AUD share a common set of neurobiological mechanisms (Wichniak, Wierzbicka et al. 2013) often manifesting as increased REM duration, shorter REM latency, and increased REM density (Roehrs and Roth 2001, Pittenger and Duman 2008, Colrain, Nicholas et al. 2014, Roberto and Varodayan 2017, Riemann, Krone et al. 2020). Given the reciprocal relationship between REM and NREM (Kupfer and Ehlers 1989), these markers of REM-hyperactivity in MDD and AUD are often accompanied by NREM hypoactivity (Irwin, Gillin et al. 2002), principally in the form of attenuated slow wave activity (SWA), a highly synchronized, oscillatory brain state responsible for synaptic homeostasis and brain network modulation (Dijk, Brunner et al. 1990). MDD and AUD demonstrate lower SWA across the night and lower delta sleep ratios (DSRs: (The ratio of Delta or SWA in the 1st relative to 2nd NREM Cycle) than normal sleepers, both of which are indicative of insufficient homeostatic sleep drive (Kupfer, Frank et al. 1990, Lotrich and Germain 2015).

Sleep therefore represents an important consideration in the evaluation of both MDD and AUD interventions. Despite this, sleep neurophysiology and architecture have largely been overlooked in studies involving psilocybin administration in either healthy participants or individuals with MDD and/or AUD. Only one small study in healthy humans (Dudysová, Janků et al. 2020) examined the effects of psilocybin administration on sleep, reporting prolonged REM latency following a single daytime administration. However, REM density, DSR, and other key biomarkers for MDD, were not explored. The same study also reported a reduction in delta power during SWS in the first NREM sleep cycle, suggesting alterations in homeostatic sleep drive, but did not investigate the temporal dynamics of SWA across the night, a phenomenon which holds greater clinical relevance given its association with depression-related outcomes. It is also not known whether these effects extend to clinical populations. Prolongation of REM latency has equally been observed in animal models (Thomas et al., 2022), coupled with enhanced oscillations in the delta frequency band, following administration of psilocin (the pharmacologically active metabolite of psilocybin) in mice.

To our knowledge, no study has investigated whether sleep effects are sustained beyond acute administration periods, or whether objective sleep-EEG differences are observed in participants receiving psilocybin within the context of clinical intervention. Therefore, we aimed to conduct the first prospective study examining treatment effects of PAT on sleep in a sample of participants with comorbid MDD and AUD. We collected sleep-EEG for 10 consecutive nights, spanning both pre-treatment (Nights -2 to 0) and post-treatment (Nights +1 to +7) periods anchored to a session of PAT, and assessed changes in sleep neurophysiology and architecture with documented mechanistic relevance to both MDD and AUD.

Methods

Hypotheses

Based on prior findings, we hypothesized that psilocybin would result in changes in the sleep-EEG profile indicative of an increased NREM homeostatic sleep drive (e.g., increased SWA/delta power and DSR) and a reduction in markers of REM-hyperactivity (e.g., reduced REM density: see detailed hypotheses Table S1).

Recruitment and Screening

The current sub-study recruited participants from a parent study assessing the efficacy of psilocybin-assisted therapy for depression in participants with comorbid MDD and AUD (NCT04620759). The parent project recruited and treated a total of 83 male and female volunteers who are between the ages of 21 and 65 years and who met Diagnostic and Statistical Manual, Fifth Edition (DSM-5) criteria for both MDD and AUD (Spanning 01/2022 to 12/2025). A total of 43 participants consented to undertake the additional sleep-EEG monitoring described here. Volunteers were recruited from the community (Through online and print advertisements) and randomized to one of two study arms (25 mg oral psilocybin vs oral placebo), with Urn stratification (Wei and Lachin 1988) used to balance depressive symptom severity (using the Quick Inventory of Depressive Symptoms, Self-Rated version, or QIDS-SR (Rush, Trivedi et al. 2003)), alcohol use (total days drinking as assessed with the Time-Line Follow Back procedure, or TLFB), age as continuous variables, and sex as a binary variable (M | F). Randomisation was performed by an independent study team member who had no interaction with participants. Personnel responsible for screening and enrolling participants had no access to the randomisation system or treatment assignments before allocation. The parent protocol involved two psilocybin administration sessions, one placebo controlled (Session 1) and one open-label (Session 2), paired with Motivational Interviewing for alcohol use. The present analyses report findings solely from the placebo-controlled session (Session 1). Participants underwent assessments of depression (QIDS-SR as well as a blinded, clinician-rated GRID-HAMD (Williams, Kobak et al. 2008)) and alcohol use (using the TLFB) before treatment to establish eligibility and inform stratification. The full inclusion/exclusion criteria for the parent protocol are listed in Supplementary Materials (Table S2).

Procedure

We present here a pre-registered quadruple-blind (Participant, Care Provider, Investigator, Outcomes Assessor) secondary analysis of data from a randomized, placebo-controlled clinical trial (Clinical trials.gov identifier: NCT04620759, OSF: https://osf.io/v4825) that took place at the Johns Hopkins Center for Psychedelics and Consciousness Research (CPCR). The study was approved by the Johns Hopkins Medicine Institutional Review Board (IRB), and all participants provided written informed consent prior to participation. The study was conducted in accordance with the approved protocol and applicable ethical guidelines, and the funder did not participate in study design or execution. The trial was conducted and reported in accordance with the Consolidated Standards of Reporting Trials (CONSORT) guidelines (see CONSORT checklist in supplement). Patients and members of the public were not involved in the design, conduct, analysis, or reporting of this study. Participants who enrolled in the current sub-study underwent at-home sleep measurements using a portable wireless sleep-EEG device (Sleep Profiler X8) for three nights pretreatment and seven nights post treatment, relative to the experimental drug administration. Objective sleep parameters (NREM and REM spectral power, sleep duration, continuity, and sleep architecture) were measured each night.

[insert figure 1 here]

We elected to conduct seven nights of sleep-EEG post administration to mitigate any EEG effects resulting from psilocybin metabolites and transient alterations in receptor trafficking that occur immediately following administration (Brown, Nicholas et al. 2017, Doss, Považan et al. 2021), and to align with our aim of assessing psilocybin's enduring effects on sleep. Prior to their drug sessions, participants were trained in the self-administration of the wireless at-home EEG device according to an existing and well-validated protocol (Reid, Dunn et al. 2024). Participants were provided with a detailed instructional manual and a video explaining these procedures and completed three nights of sleep assessments leading up to the day of their drug-administration, and seven subsequent nights beginning the night following drug administration. See Table S3 for detailed summary of sleep events

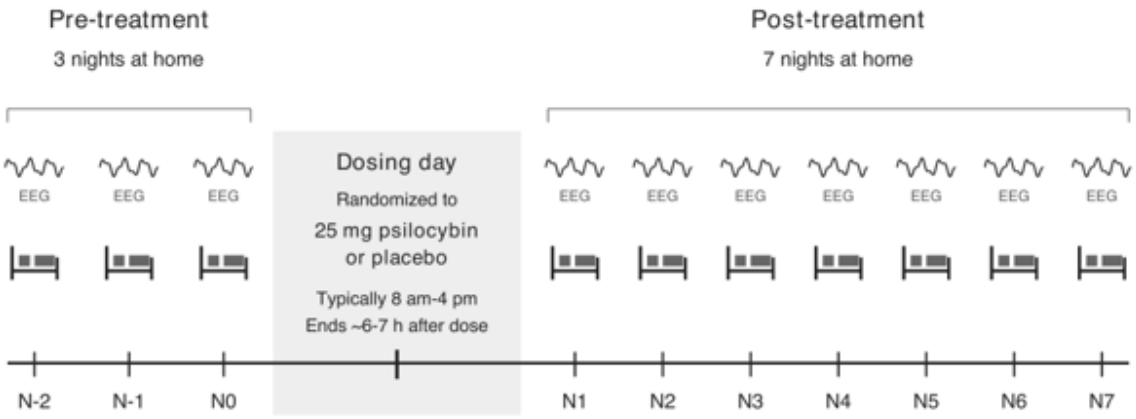


Figure 1: Study Design: Participants with comorbid major depressive disorder and alcohol use disorder completed three nights of home-based sleep electroencephalographic (EEG) monitoring before treatment (N−2, N−1 and N0) and seven nights after treatment (N1–N7). During the intervening dosing day, participants received either 25 mg oral psilocybin or placebo under monitored conditions. Dosing sessions typically occurred between 08:00 and 16:00, concluding approximately 6–7 hours after administration. N0 denotes the night immediately preceding dosing, and N1 denotes the first night following dosing. Each EEG and bed symbol represents one scheduled overnight recording, used to assess spectral activity, sleep architecture and sleep continuity across the pre-treatment and post-treatment periods

Drug administration procedures

Drug administration was conducted at the CPCR following best practices for research administration of psilocybin (Johnson, Richards et al. 2008) in three phases: 1) *preparation*, 2) *medication administration under monitored and controlled conditions*, and 3) *aftercare*, as explained below.

Phase 1 (preparation): After screening and enrollment, participants met with study team members trained in psilocybin administration on at least two separate occasions, totaling eight hours of preparation. The main purpose of these meetings was to develop rapport and trust, which minimizes risks associated with fear or anxiety reactions that may occur during the drug administration sessions. Participants engaged in a life review, including a focus on important events and milestones in their life. Study team members described and prepared the participant for the possible range of experiences that can be encountered in a psychedelic therapy session, including strong positive and negative emotions as well as substantial changes in perception, cognition, and consciousness. Participants were given a chance to practice what happened in phase 2 (e.g., lying on a couch with eyeshades and headphones and listening to music). Participants also engaged in a brief 45-minute motivational interviewing intervention, led by a trained and independently licensed therapist.

Phase 2 (experimental drug administration under monitored and controlled conditions): Urine tests for illicit drugs and pregnancy were completed upon arrival; negative screening results were required to continue. Blood pressure and heart rate were determined to be normotensive before drug administration to minimize risk of hypertensive reaction to psilocybin. Participants swallowed an identical capsule containing either placebo (microcrystalline cellulose) or an oral dose of psilocybin (25 mg) under observation. Participants then lay down on a couch after donning eyeshades and headphones and listened to a standardized program of music (see (Davis, Barrett et al. 2021) for full list), whilst being instructed to turn inward and be present for the experience. Two trained study team members (at least one licensed clinician) remained with the participant throughout the session. Blood pressure, heart rate, and staff ratings of participant behavior (e.g., drug effect strength, anxiety) were assessed throughout the session to monitor participant safety. At the end of each drug administration session (~6-7 hours after treatment, and after drug effects subsided), participants met with a study team investigator and the two study team members who monitored their session, to ensure safety and resolution of any acute drug effects before being released into the care of a pick-up person identified by the participant prior to the drug administration session.

Phase 3 (aftercare): Each participant followed up with study staff, either in person, via phone, or via secure video conference, during the days and weeks after each drug administration session to discuss their experiences. During these post-session visits, study staff monitored and reviewed adverse events, and study staff and participants revisited the experiences encountered during the medication administration session.

EEG Procedures

EEG data collection: Sleep-EEG data were collected in participants' homes, opposed to a sleep-laboratory setting, as many participants report mild discomfort associated with the use of traditional in-lab polysomnography and sleeping for the first night in an unfamiliar environment is associated with reduced sleep depth, quality and increased awakenings, i.e. a 'First-night effect' (Tamaki, Nittono et al. 2005). Best practice for in-laboratory sleep-EEG involves an additional adaptation night. However, the use of an at-home wireless EEG device minimizes invasiveness and participant burden by reducing the requirement for an adaptation night (Levendowski, Ferini-Strambi et al. 2017).

Data were collected using an ambulatory wireless sleep-EEG device (Sleep Profiler X8, Advanced Brain Monitoring, Carlsbad CA). This device has been validated against the gold standard (Polysomnography) method of measuring sleep architecture (Finan, Richards et al. 2016). EEG data are collected from three EEG electrodes (FPz, AF7, AF8) located on the forehead. The device was self-administered in participants' homes using disposable EEG electrodes. Participants were trained in how to correctly apply the device and initiate recordings.

Prior to hypothesis testing, we tested for the presence of a first night effect by testing differences in total sleep time (TST), wake after sleep onset (WASO), and sleep efficiency (SE) between N+1, N+2 and N+3 using repeated-measure ANOVA tests and pairwise contrasts with post-hoc Tukey HSD corrections (Tables S4-S5). Across variables, no evidence of a first-night effect was observed. Further, due to our randomized design, we did not anticipate any systematic impact of a first-night effect on our ability to detect between-group differences. Therefore, we proceeded to include all 10 nights in statistical analyses.

Sleep scoring: Raw Sleep EEG data were reviewed and manually scored by a Registered Polysomnography Technician (RPSGT) at the Johns Hopkins Center for Interdisciplinary Sleep Research and Education (CISRE) who remained blind to drug allocation. Scoring of sleep related events (Sleep Stages N1, N2, SWS, REM) was conducted

in accordance with V3.0 of the American Academy of Sleep Medicine (AASM) scoring manual (Troester MM. 2023). Each record then underwent further blind review by a Board-Certified Sleep Medicine Physician before being released, without condition labels, to the EEG analyst (MJR) for blind quantitative EEG analyses.

EEG preprocessing: Preprocessing and analysis were performed using MATLAB (R2025b), and R (V4.6.1) on the raw European data format (EDF) files. XML scoring files provided auxiliary markers of sleep-stage scoring by the RPSGT. We first removed records/nights in which signal quality issues were non-permissive for scoring or signal processing (as identified by the RPSGTs during scoring). We also removed epochs with other scored events likely to obscure EEG power estimates (i.e. major body movements). We then identified the timespan of any arousals or artifacts from the scoring labels and removed data between the start and end bounds of the arousal periods +/− 3 seconds to account for any transitionary artifacts. Raw data, post-artifact removal, were imported into MATLAB, and the 30-second epochs labeled as NREM (either N1, N2, and N3) were isolated from wake and REM epochs and concatenated. We further preprocessed data from NREM (Concatenated N+1, N+2 & N+3) and REM epochs in separate time series. Data were then zero-phase high-pass filtered at 0.5 Hz to retain the temporal structure of the data using a Finite Impulse Response (FIR) filter with a stop band frequency of 0.1Hz and subsequently notch filtered using an infinite impulse response filter (IIR) at 60 Hz to remove geographically specific (USA) electrical line noise. We next followed a documented and well-validated pipeline (Purcell, Manoach et al. 2017, Mariani, Tarokh et al. 2018) to automatically reject remaining artifacts consisting of the following steps: (1) the removal of clipped epochs, defined as epochs in which 5% of the signal amplitude values were clipped at the maximum amplitude value; (2) performing a first-pass Welch's Fast Fourier Transformation (FFT), windowed with a 4-second sliding Hamming window (50% overlap), to calculate first-order approximations of delta (0.5–4 Hz) and beta (18–30 Hz) power spectral density across a moving average of 15 contiguous epochs. Epochs exceeding >2.0 times (for beta-band power spectral density, or PSD) or > 2.5 times (for delta PSD) the local average of 15 epochs were removed. These spectral procedures were used exclusively for artifact rejection, not empirical analyses (see "Spectral analyses" below). We then rejected residual artifacts by classifying the root mean square values and three Hjorth parameters (activity, mobility, and complexity (Hjorth 1970)) for 30-second epochs and rejecting those that were > 2.5 times the median for each parameter. Epochs and time segments of data that were removed by automatic processing were retained and visualized to confirm their status as artifacts to be removed from analyses and not sleep physiological phenomena otherwise classified as artifacts. We next plotted the whole-night spectrogram for each participant-night to identify records in which non-biological signal contamination remained. These files underwent further visual rejection of artifacts using the EEGLAB toolbox, after which they were reprocessed according to the above procedures. After this final step, files that were considered of insufficient quality were rejected from the analysis set entirely.

Spectral analyses

Following the preprocessing procedures described above, we performed multitaper spectral decomposition on the preprocessed EEG signal. Given that our goal was to assess whole-night phenomena, temporal precision was of minimal concern, and we adjusted the parameters accordingly to maximize frequency resolution (the precision of our 0.5-2Hz PSD, estimates – our lowest frequency of interest) and minimize spectral leakage from neighboring frequencies. Therefore, we used 0.125 Hz frequency resolution of NREM power to capture a time course of spectral power across the frequency range of 0.5–35 Hz (total 277 frequency bins) for each night, using an 8-second sliding window with a step size of 1 second and a time-half bandwidth of 3, with the number of orthogonal Slepian tapers set to 5, according to:

$$\Delta f = \frac{1}{T}$$

$$TW = T \cdot W$$

$$K = 2TW - 1$$

Where T = window length, Δf = frequency resolution, TW = the time-half bandwidth and K = the number of orthogonal tapers. All tapers were uniformly weighted. Data were first de-trended to remove the low-frequency DC component, and then multiplied by each of the Discrete Prolate Slepian Sequence (DPSS) tapers before computing the Short-time Fast Fourier Transforms (FFTs) for each tapered segment:

$$X_k(f) = \sum_{t=0}^{N-1} x(t) v_k(t) e^{-i2\pi ft}$$

PSD estimates for each taper were conducted by summing the squares of the real and imaginary parts generated by the tapered FFTs. The one-sided PSD spectrum of the averaged tapers was calculated by multiplying the values between the DC component and the Nyquist frequency (128Hz) by two to resolve negative frequency values into real-valued power estimates of positive-frequencies and divided by the sample frequency (f_s = 256 Hz) to normalize PSD in terms of power per unit frequency for each epoch.

$$\widehat{S_1}(f) = \frac{2}{K f_s} \sum_{k=1}^{K} |X_k(f)|^2$$

The mean spectrogram of each of these tapers was then calculated to compute the one-sided PSD spectrum for each 8s window. Extreme PSD values outside the 5th to 95th percentiles were rejected. These values were then median-aggregated across the night to calculate average whole-night PSD values for each canonical band whilst limiting the influence of outlier epochs. We computed PSD across the canonical (Troester MM. 2023) SWA (0.5-2Hz), delta$_2$ (2-4Hz), theta (4-8Hz), alpha (8-13Hz), sigma (13-16Hz), and beta (16-35Hz) powerbands. Although the original preregistration specified delta power as a single canonical frequency band encompassing both SWA and delta$_2$, these frequency ranges were analysed separately in the present study to account for established differences in their underlying physiology and functional correlates. For REM PSD estimates, we omitted SWA and delta$_2$ from statistical analysis as these are highly contaminated by eye-movement artifacts complicating interpretation of PSD values. We had no hypotheses concerning the topographical effects of these PSD values, and therefore, to reduce the number of comparisons, we used only the average PSD for both AF7-Fpz and AF8-Fpz electrodes as our outcome.

Rem Density: REM Density was calculated as the mean number (#/30s epoch) of REMs, calculated from all epochs of phasic REM. REM epochs were determined by RPSGT scoring, but individual REMs were detected using an established automated procedure (Levendowski, Ferini-Strambi et al. 2017). Slow eye rolls and phasic REMs were distinguished using Pearson correlations of AF7–Fpz and AF8–Fpz signals following 6.5 Hz zero-phase IIR filtering. Delta power arising from phasic REM versus SWS was differentiated by comparing filtered and unfiltered Delta^C, defined as delta-band (0.5–4 Hz) power corrected for ocular activity (with a median filter). Epochs with high beta power and low EMG activity were classified as tonic REM and distinguished from tonic stage N1 based on their temporal proximity to phasic REM epochs. Brief, transient increases in EMG activity (e.g., <5 seconds) typically resulted in classification as wake.

Delta Sleep Ratio: DSR was calculated according to standard procedures (Nissen, Feige et al. 2001) as the ratio of absolute delta-band (0.5–4 Hz) power spectral density (μV^2/Hz) in the first NREM cycle relative to the second NREM cycle. NREM cycles were computed using an automated custom algorithm written in MATLAB. The first NREM cycle (NREM1) was defined as ending at the onset of six consecutive 30-second REM epochs (REM1) (Nissen, Feige et al. 2001). The second NREM cycle (NREM2) was defined as beginning at the first occurrence of six consecutive non-artifactual NREM epochs following REM1 onset and ending at the onset of the subsequent sequence of six consecutive REM epochs (REM2). To ensure cycle validity and limit incomplete cycle detection, NREM2 was required to have a minimum duration of ≥20 minutes prior to REM2 onset. Nights during which no REM1 was detected were not considered for DSR calculations. Instances in which a REM1 period was detected, but no REM2 period was detected were operationalised by defining NREM2 as beginning at the end of REM1 and terminating after A) the same duration as NREM1 elapsed or B) the end of the sleep period, depending on which occurred first. Spectral analyses (see section above) were then performed independently for NREM1 and NREM2 on each of the two EEG channels. Whole-night hypnograms and individual-cycle spectrograms were examined to identify signal artifact, or algorithmic error in cycle determination, and manual override procedures followed as necessary to ensure correct cycle extraction. If artifact remained in any of the four segments (i.e., NREM1/2 × left/right channels), the segment(s) were marked to be rejected and DSR was calculated only on the non-artifactual segments. Finally, when values were available for all four segments DSR was calculated as the mean of (abs[NREM1-R] / abs[NREM2-R]) & (abs[NREM1-L] / abs[NREM2-L]). In cases where a single segment (i.e NREM2-L or NREM2-R) was rejected, the mean of the intact cycle's components (i.e. NREM1 = mean[NREM1-R, NREM1-L]) was first calculated prior to DSR calculation (i.e. mean[NREM1] / mean[NREM2]). To provide a point of comparison with the prior psilocybin study (Dudysová, Janků et al. 2020) we also examined SWA during the first NREM cycle as an independent sensitivity analysis.

Statistical Approach

Blinding Procedures

Analysis was performed by MR, who was blinded to participant allocation throughout data-collection and analysis. As the baseline sleep assessment took place prior to randomization, baseline assessments were conducted in an appropriately double-blind manner. Nonetheless, as we focused on objective outcomes, our analyses were less likely to be influenced by functional unblinding. To facilitate blind data-analysis, a research coordinator provided a list of anonymized participant IDs and blinded group allocations (e.g., Group 1, Group 2). To limit reporting bias, the analyst did not interact with any study participants either during or after study procedures, and no discussions of participant experiences occurred between MJR or any study team members through to the end of analysis. Further, MJR was only unblinded to drug allocation after primary analyses were finalized and the results of the statistical analyses were written.

Sample size and power calculations

Sample size calculations were performed using G*power (Faul, Erdfelder et al. 2009), separately for each outcome based on effect sizes reported in the literature (see table S1). Overall, it was estimated that a total sample size of 43 participants would achieve 95% power to detect a moderate effect (estimated d = 0.49 - 0.84; (Dudysová, Janků et al. 2020) with two-sided $\alpha = 0.05$ for all main outcomes). The parent study enrolled and treated 83 participants, of which 43 consented to complete the sleep-EEG monitoring described here. No early stopping rule was applied, and interim data analyses were not conducted.

Statistical Analyses

Multilevel Random Effects Models (MLMs) were used to assess whether psilocybin alters EEG PSD in each canonical frequency band across time, to investigate whether psilocybin increased PSD post-treatment relative to placebo. MLMs were also used to assess whether psilocybin increased REM latency or reduced REM density relative to placebo. Univariate normality was assessed by descriptive statistics with skew > |3| or kurtosis > |10| considered problematic. Model residuals and Q-Q plots were visually inspected to confirm core model assumptions including residual normality, homoscedasticity, influential observations, multicollinearity, and the distribution of random effects. Cook's distance was calculated for each model to identify observations that influence the model results (*i.e.,* leverage points). Models were analyzed both with and without leverage points included in the model to understand whether the results were influenced by a few unique cases. Assumptions were first evaluated by comparing variance components from null and conditional models. Through this process, maximum likelihood estimation was used to evaluate model fit. A participant level random intercept was included to account for random variability in the outcome measures at baseline, and restricted maximum likelihood was used to fit final statistical models. Statistical analyses were performed in R (version 4.6.1) using the lme4 and lmerTest packages for linear mixed-effects modelling, the splines package for natural cubic spline functions, ggeffects for model-based predictions, emmeans for estimated marginal means and post-hoc contrasts, and refund for functional-on-scalar regression.

As the raw spectral and architectural values evidenced non-linear trajectories across the study period, we incorporated natural cubic splines to flexibly model nonlinear trajectories over time. Night (treated as a continuous variable) was modeled using a natural spline basis with 3 degrees of freedom, allowing for smooth, non-monotonic changes without imposing a strictly linear or polynomial structure. This approach yielded three spline basis coefficients that jointly parameterize the nonlinear trajectory across nights. For each outcome, models included fixed effects for the spline-transformed night variable, group, and their interaction, such that uncorrected analyses followed the convention:

$$outcome \sim ns(night, df = 3) \times group + phase + (1 \mid participant)$$

$$Y_{ij} = \beta_0 + \sum_{k=1}^{3} \beta_k S_k(night_{ij}) + \beta_4 group_i + \sum_{k=1}^{3} \beta_{4+k}\left(S_k(night_{ij}) \times group_i\right) + \beta_8 phase_{ij} + b_{0i} + \varepsilon_{ij}$$

For clarity, covariates included in the fitted models are omitted from the model specifications above. This parameterization allowed us to test whether trajectories over time differed between groups, whilst accounting for baseline differences via the main effect of group. The inclusion of spline terms enabled the model to capture curvilinear patterns, such as delayed or transient effects following drug administration, which would not be detected using linear time terms. Spline coefficients were evaluated individually to identify group differences in specific components of the nonlinear trajectory, while model-derived predicted values were used to characterise the direction and temporal pattern of these differences. Estimated marginal means and predicted trajectories were generated and visualized to aid interpretation of temporal patterns. This approach was selected to balance flexibility and parsimony, given the relatively small sample size, whilst allowing detection of nonlinear, time-dependent effects following dosing. MLMs with participant-level random intercepts were used to examine the evolution of spectral power over time, modeled using spline basis functions, group differences, and their interaction, adjusting for age, race, sex, depressive symptom severity (SR-QIDS), and alcohol use (TFLB).

As mixed effects models are implicitly robust to instances of missing data, no imputation was performed. We obtained robust and stable estimates of the 95% Confidence intervals for all fixed effects by using resampling performed through a bootstrapping procedure (2000 bootstraps). Finally, following first-pass completion of analysis, the analysis code and raw data were reviewed by a third-party investigator with no direct involvement in the study (CD). All statistical codes are readily available as Supplementary Materials and online on the project's Open Science Framework page (https://osf.io/v4825/).

Whilst it is possible that the pharmacological properties of psilocybin may exhibit direct effects on sleep architecture, an alternative hypothesis is that reductions in depressive symptoms or alcohol use that occur in response to psilocybin-assisted therapy could, indirectly, alter sleep architecture. Whilst the current study was underpowered to statistically test such mediational pathways, and this was not our primary goal, Pearson's correlation coefficients were calculated to understand whether changes in depressive symptoms or alcohol use are correlated with alterations in sleep architecture. Correlations were calculated using only those participants who received psilocybin-assisted therapy. Treatment-related changes in alcohol use (total # of drinking days measured with the TLFB), depressive symptoms (measured using GRID-HAMD), and sleep architecture were calculated using change scores (pre – post). Correlational analyses should be interpreted with caution and used to generate hypotheses for future mechanistically focused studies.

Multiplicity correction: Primary inference was based on nominal model-derived *p*-values for the prespecified sleep outcomes. The spectral and sleep-architecture outcomes were not statistically or physiologically independent: relative spectral powers represent components of the same normalized spectrum and are therefore inherently interdependent, while sleep-architecture measures similarly quantify related and, in some cases, mathematically overlapping aspects of the same sleep period. Accordingly, these outcomes were considered a structured set of related measures rather than independent tests of unrelated hypotheses. Nevertheless, to assess the robustness of the primary findings to multiplicity across related outcome measures, supplementary analyses were performed using the Benjamini–Hochberg false discovery rate (BH-FDR) procedure. Multiplicity was defined across prespecified outcomes within each analysis domain, rather than across the three coefficients arising from the natural cubic spline representation of night. Specifically, BH-FDR correction was applied across six NREM spectral outcomes (slow-wave activity [SWA], $delta_2$, theta, alpha, sigma, and beta), four REM spectral outcomes (theta, alpha, sigma, and beta), and 11 sleep-architecture outcomes. Because the three spline basis coefficients represent distinct components of the nonlinear trajectory, group-by-spline interactions were evaluated at the coefficient level. Multiplicity was controlled across prespecified outcomes for each corresponding spline component, rather than across all spline coefficients collectively, using separate BH-FDR corrections for spline components 1, 2, and 3. Statistical significance following multiplicity correction was defined as a BH-FDR-adjusted $p < .05$.

Exploratory analyses

Correlations between sleep changes and clinical outcome: Among participants receiving psilocybin, linear slopes across the seven post-administration nights were calculated for each spectral measure to quantify individual changes in sleep neurophysiology. Pearson correlations were used to examine associations between these slopes and changes in depressive symptoms (GRID-HAMD; baseline to 1 month post-administration) and alcohol use (percentage drinking days and mean drinks per day; baseline to 3 months post-administration). To minimise potential overlap

between objective spectral sleep measures and sleep-related symptoms captured by the HAM-D, sleep-related items were excluded from the HAM-D score used in these analyses.

Examining interactions between trajectories of spectral bands: Given the temporal patterns observed in SWA and sigma power in the primary analyses, we conducted a post hoc analysis to explore whether their trajectories were related. Contemporaneous sigma power was included as a moderator of the non-linear relationship between study night and SWA, with interactions evaluated for each natural spline basis function.

Function on Scalar Regression Analyses: To evaluate treatment-related differences across the continuous EEG power spectrum without imposing a priori frequency-band boundaries, we performed functional-on-scalar regression (FOSR) using the refund package in R. Spectral power at each frequency was log10-transformed and treated as a functional outcome, with treatment group entered as a scalar predictor. Models were estimated using ordinary least squares with 20 basis functions, yielding a treatment-group coefficient function representing the estimated difference in log10 spectral power between groups as a function of frequency.

Because repeated nightly observations were available for each participant, uncertainty in the estimated treatment effect was quantified using a participant-level cluster bootstrap. Participants were resampled with replacement separately within each treatment group, with all available nightly observations from each selected participant retained together in each bootstrap sample, thereby preserving the within-participant dependence structure and randomized group allocation. The FOSR model was refitted to each of 2,000 bootstrap samples, and pointwise 95% confidence intervals for the treatment-group coefficient function were calculated from the 2.5th and 97.5th percentiles of the resulting bootstrap distributions at each frequency. Frequency regions in which the pointwise 95% confidence interval excluded zero were identified as regions showing evidence of between-group differences. Missing spectral values were interpolated before model fitting using the median spectral power at the corresponding frequency within treatment group. The primary coefficient function was estimated from all available participant-night observations after imputation, while resampling-based inference accounted for clustering of repeated observations within participants.

Results

Sample Characteristics

43 participants were randomized and completed the at-home sleep assessments. Data from three participants were excluded as they did not receive the study drug – See CONSORT flow in Figure S1. Data from 40 participants (placebo: n = 18 | psilocybin: n = 22) were therefore included in the analyses. Baseline demographic and clinical characteristics were generally balanced across groups. Participants had a mean age of 44.4 years (SD = 10.9) and were predominantly White/Caucasian (92.5%). The psilocybin group included a greater proportion of females (63.6% vs 38.9%), whereas the placebo group included a greater proportion of males (61.1% vs 36.4%). Slightly more participants in the psilocybin group were maintained on antidepressants than in the placebo group (40.9% vs 33.3%). Baseline depressive symptom severity was similar between groups on both the QIDS-SR (placebo: 15.7 ± 4.17; psilocybin: 16.6 ± 3.79) and GRID-HAMD (placebo: 21.3 ± 4.73; psilocybin: 21.5 ± 4.72). Subjective sleep quality was also comparable (placebo: 9.06 ± 3.25; psilocybin: 8.42 ± 2.59) and indicated generally poor sleep quality. Alcohol use characteristics, including heavy drinking days, regular drinking days, abstinent days, and drinking quantity measures, showed minimal differences between groups. Overall, no notable baseline imbalances were observed, supporting successful randomization (Table 1). No adverse events or serious adverse events occurred in either the psilocybin group or the placebo group during the study period.

Sleep macrostructure and continuity variables at baseline

In total, we collected 305 person-nights of recordings from 40 participants. Eight of these nights (2.6%) were removed due to irresolvable signal artifact (placebo: n = 2 nights | psilocybin: n = 6 nights). The average number of total nights for each participant was 8. The average number of nights pre-dose was 3 and the average number of nights post-dose was 5.

Across the full sample, participants spent an average of 433.4 ± 88.4 *mins* in bed and obtained 369 ± 116 *mins* of total sleep time, with a mean sleep efficiency of 85.5 ± 17.4%. Mean sleep onset latency was 17.6 ± 22.6 *mins* and REM latency was 88.0 ± 51.1 *mins*. Participants spent an average of 31.8 ± 28.8 *mins* awake after sleep onset (WASO). Sleep architecture consisted of 6.89% NREM1, 49.8% NREM2, 20.1% SWS, and 23.2% REM. Baseline

sleep measurements were broadly comparable between placebo and psilocybin groups, although the psilocybin group exhibited somewhat longer sleep onset latency (23.0 vs 13.5 *mins*) and slightly lower sleep efficiency (83.3% vs 87.1%), relative to placebo – See Table 2.

First-night effect

Before proceeding with inferential analyses, we examined whether there was evidence of a first-night effect, reflecting potential alterations in sleep duration (TST), continuity (WASO, SE) and spectral characteristics (NREM and REM PSD) arising from unfamiliarity with the sleep-EEG equipment. Analyses across Nights 1–3 demonstrated no significant effect of recording night (all $p > .10$ – Table S4), with Tukey adjusted estimated marginal mean contrasts further indicating no significant differences between individual nights (all $p > .09$ – Table S5). We therefore proceeded with analyses including all available nights.

Primary Analyses: NREM Spectral power

Across frequency bands, there was consistent evidence of nonlinear change in spectral power across nights. When collapsed across both groups, no significant evidence of nonlinear change in spectral power across nights was observed, as evidenced by non-sufficient fixed effects (Table 3). Critically however, temporal dynamics differed between groups, as evidenced by significant group × night interactions for SWA ($b = 5.48$, $p = 0.032$), and sigma power ($b = -5.88$, $p = .025$), driven by the third spline basis component, indicating that group differences were not constant but instead emerged as differences in the shape of the nightly trajectories. SWA and sigma produced sigmoidal trajectories that appeared to be coupled in antiphase, with increasing SWA corresponding to decreasing sigma power for the first four nights in the psilocybin group, and the opposite pattern in the placebo group – Figure 2. Subsequently, local maxima (sigma) and minima (SWA) occurred on night 4 (+ 4 nights from dosing) for the psilocybin group, followed by increasing SWA and decreasing sigma towards night seven. In contrast, there was no evidence of group differences in the temporal dynamics of $delta_2$, theta or beta power (all interactions $p > 0.15$ – See Table 3). These effects are reflected in the trajectory patterns shown in Figure 1. Fixed effects of group were not statistically significant for any frequency band (all $p \geq 0.08$), suggesting that differences between groups were driven primarily by divergence over time rather than overall mean differences. Nested model comparisons performed via ANOVA demonstrate that equivalent linear models did not improve model fit for any outcome–Table S6. Similarly, sensitivity analyses conducted after removing outliers via Cook's distance parameterization did not materially alter the outcome of the analyses – Table S7.

[insert figure 2 here, p13]

REM Spectral Power

Evidence for nonlinear change across nights was present in specific frequency bands but was less consistently observed across the spectrum. Significant fixed effects of the third spline basis were identified for sigma power ($b = 9.81$, SE = 3.91, $p = .013$), and beta power ($b = 0.48$, SE = 0.15, $p = 0.002$), indicating that spectrotemporal dynamics in REM also deviated from linear trajectories. As in NREM, there was little evidence for overall group differences in mean spectral power (all $p > .20$). However, differences in temporal dynamics were again evident. Significant group × night interactions were observed for sigma ($b = -6.82$, SE = 2.67, $p = 0.011$), and beta power ($b = -0.31$, SE = 0.11, $p = 0.003$ – see table 4), indicating that in the psilocybin group followed curvilinear increases from baseline, peaking three nights after psilocybin administration and subsequently declining across the following nights, whereas the placebo group was relatively in the post-acute period (see figure 3 - below). In contrast, no evidence of nonlinear change or group-dependent temporal dynamics was observed for, theta, or alpha power during REM (all $p \geq 0.06$ – see table 4). Nested model comparisons performed via ANOVA demonstrated that equivalent linear models for each outcome either did not improve model fit (theta, alpha, sigma) or led to significantly poorer model fit (beta) (Table S6). Sensitivity analyses conducted after removing outliers via cook's distance parameterization did not materially alter the outcome of the analyses – Table S8.

[insert figure 3 here, p14]

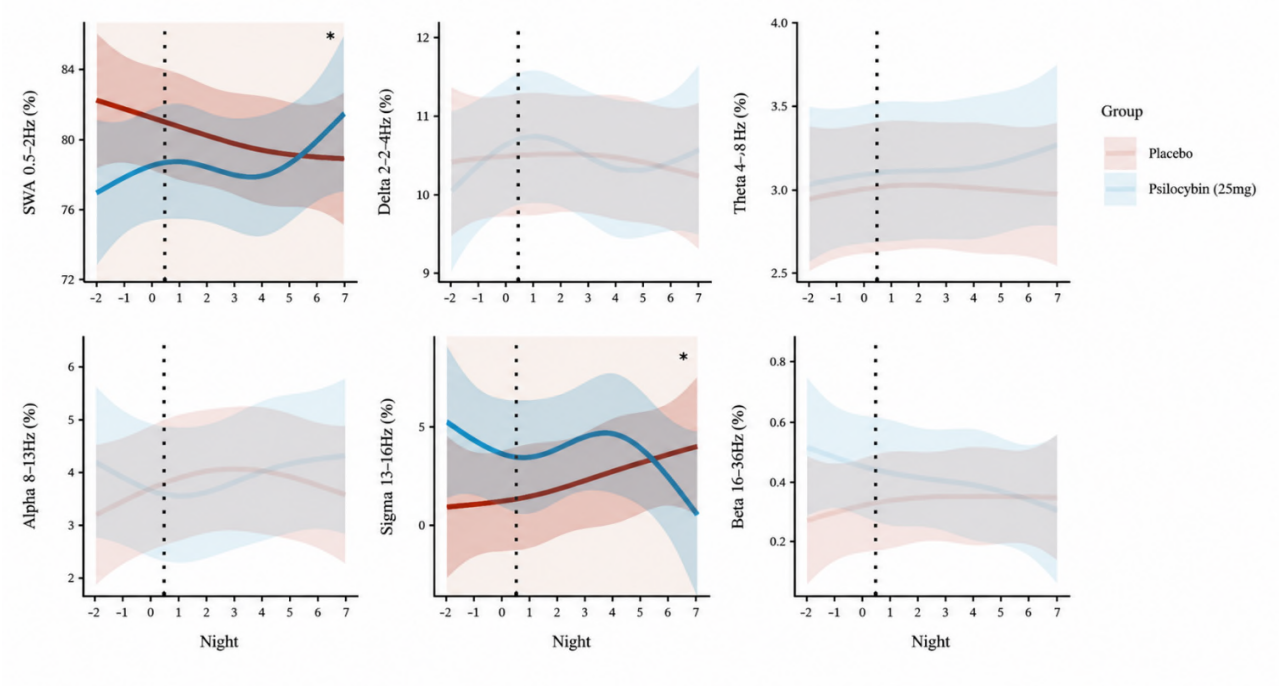


Fig. 2 Temporal trajectories of NREM spectral power before and after psilocybin administration. Panels show model-predicted relative spectral power (%) during non-rapid eye movement (NREM) sleep for slow-wave activity (SWA; 0.5–2 Hz), delta2 (2–4 Hz), theta (4–8 Hz), alpha (8–13 Hz), sigma (13–16 Hz), and beta (16–35 Hz). Trajectories were estimated using linear mixed-effects models incorporating natural cubic splines for night (three degrees of freedom), treatment group, and their interactions, with participant-level random intercepts and adjustment for age, race, sex, baseline depressive symptom severity, and alcohol use. Blue lines represent psilocybin (25 mg) and red lines represent placebo; shaded bands indicate 95% confidence intervals. Nights −2 to 0 represent pre-treatment recordings, and nights +1 to +7 represent post-treatment recordings; the vertical dotted line marks dosing between nights 0 and +1. Asterisks identify nominally significant treatment-by-night interactions for the third spline component in SWA (p = .032) and sigma (p = .025). These trajectories display approximately opposing temporal patterns, with a local SWA minimum and sigma maximum around night +4 in the psilocybin group. Faded panels indicate outcomes without nominally significant treatment-by-night interactions.

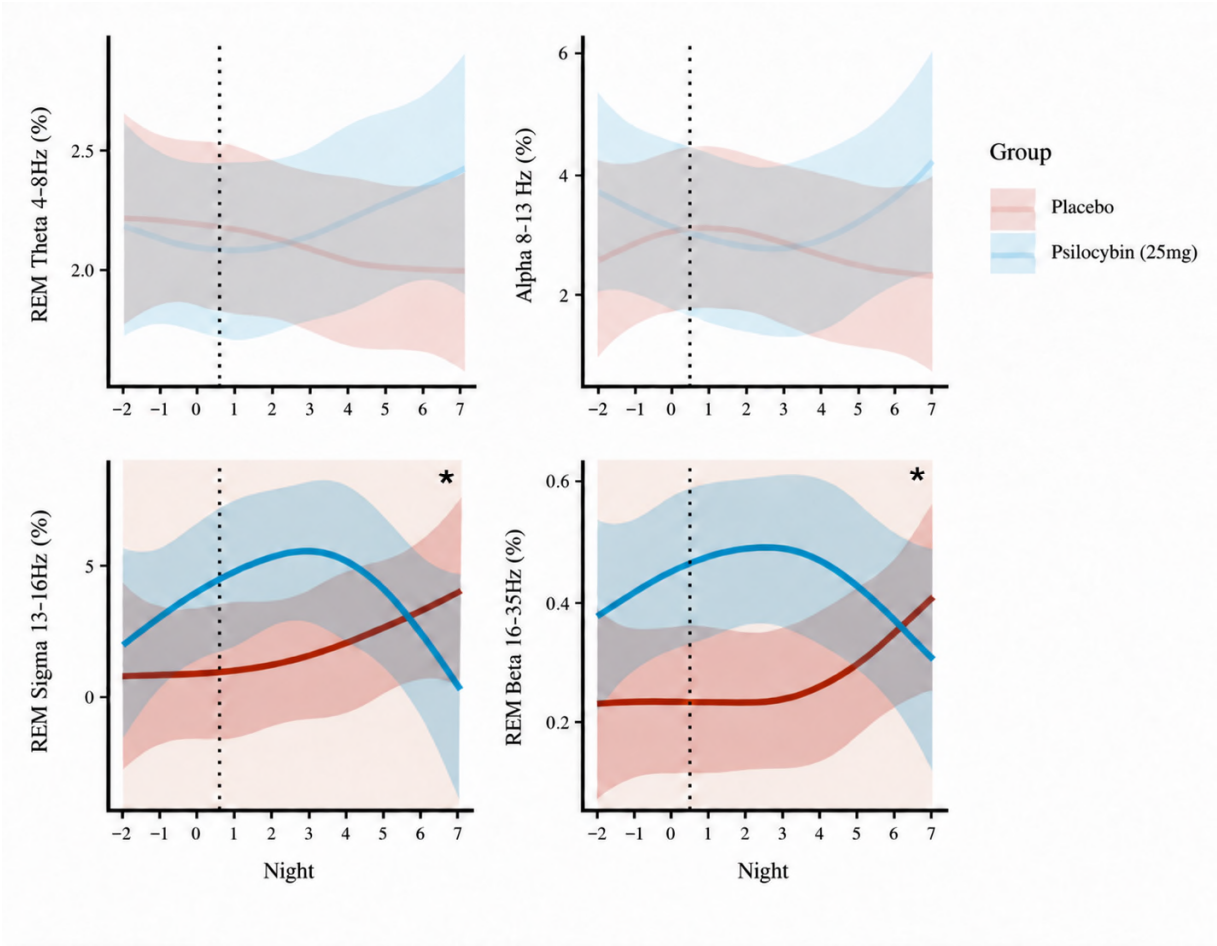


Fig. 3 Temporal trajectories of REM spectral power before and after psilocybin administration. Panels show model-predicted relative spectral power (%) during rapid eye movement (REM) sleep for theta (4–8 Hz), alpha (8–13 Hz), sigma (13–16 Hz), and beta (16–35 Hz). Trajectories were estimated using linear mixed-effects models incorporating natural cubic splines for night (three degrees of freedom), treatment group, and their interactions, with participant-level random intercepts and adjustment for age, race, sex, baseline depressive symptom severity, and alcohol use. Blue lines represent psilocybin (25 mg) and red lines represent placebo; shaded bands indicate 95% confidence intervals. Nights −2 to 0 represent pre-treatment recordings, and nights +1 to +7 represent post-treatment recordings; the vertical dotted line marks dosing between nights 0 and +1. Treatment-by-night interactions for the third spline component were significant for sigma (p = .011) and beta (p = .003), indicating differences in the shape of their temporal trajectories between groups. In the psilocybin group, predicted sigma and beta power reached local maxima approximately three nights after dosing before declining, whereas placebo trajectories increased later in the recording period.

Secondary and exploratory analyses

Sleep Continuity

Across the full sample, fixed effects of night indicated limited evidence for nonlinear changes in sleep continuity measures, irrespective of condition. SE and TST followed largely linear trajectories (all spline terms $p > .10$), except for the second spline component for TST ($b = -47.21$, SE = 21.09, $p = 0.027$). REM latency exhibited a modest nonlinear pattern ($b = 17.00$, SE = 8.93, $p = 0.07$), that did not reach statistical significance but was consistent with non-monotonic change over time. No evidence of nonlinear dynamics was observed for WASO, SOL, sleep stage composition, REM density, or DSR.

Condition-dependent differences in trajectories were evident for several outcomes, indicated by significant time × group interactions. SE showed a significant divergence between groups over time ($b = 13.76$, SE = 5.61, $p = 0.015$) for the first spline component, indicating that changes in SE evolved in a non-linear fashion across the recording period differing as a function of treatment condition. Similar group-dependent temporal dynamics were observed for TST ($b = 84.17$, SE = 44.78, $p = 0.050$) for the first spline component, suggesting that differences between conditions emerged through distinct nightly trajectories rather than overall mean differences (Table 5). In those who received psilocybin, both SE and TST increased in the four nights following psilocybin administration before declining towards baseline thereafter (Figure 4 - below). REM Latency exhibited a time × group interaction ($b = -37.07$, SE = 18.41, $p = 0.045$) with the first spline component, suggesting that REM Latency declined in the three nights following drug administration followed by a modest increasing trend thereafter. In contrast, there was no evidence of drug-dependent temporal dynamics for sleep latency (all interaction $p \geq 0.1$). WASO demonstrated a significant interaction with the second spline component ($b = -47.04$, SE = 22.06, $p = 0.034$), as well as trend-level evidence for differential trajectories between groups for the first spline component ($b = -24.46$, SE = 12.62, $p = 0.054$), alongside a similar trend for the third spline component ($b = -17.43$, SE = 10.03, $p = 0.083$), suggesting potential localized differences along the trajectory and non-uniform group differences across time. No drug-related differences were observed for SOL, sleep stage composition, REM density, or DSR. Nested model comparisons revealed that non-linear models significantly improved model fit for all outcomes relative to analogous linear models (Table S6). All models were robust to outliers determined via Cook's Distance (Table S9).

[insert Figure 4 here, p16]

Post-Acute Effects of Psilocybin (Nights 0–1 only). To examine acute changes associated with drug administration, linear MLMs were fitted comparing the night immediately before dosing (Night 0) to the night immediately after dosing (Night +1). Models included fixed effects for night (pre [Night 0] vs post [Night 1]), group, and their interaction, with participant-level random intercepts. Across spectral power during both NREM and REM sleep, there was no evidence for a fixed effect of night or a group × night interaction for any frequency band (all $p > .10$), indicating that there were no group differences in the change in spectral power between from pre- to post-psilocybin dosing. Nevertheless, significant night × group interaction was observed for SE ($p = 0.039$), demonstrating an increase in SE the first night following psilocybin administration, relative to placebo. Further trend level interactions were observed for an increase in REM duration ($p = .057$) and REM % ($p = .089$) – see tables S10-S11. For the additional sleep architecture and continuity measures including DSR and NREM-Cycle 1 SWA, there was no evidence of fixed or interaction effects (table S12).

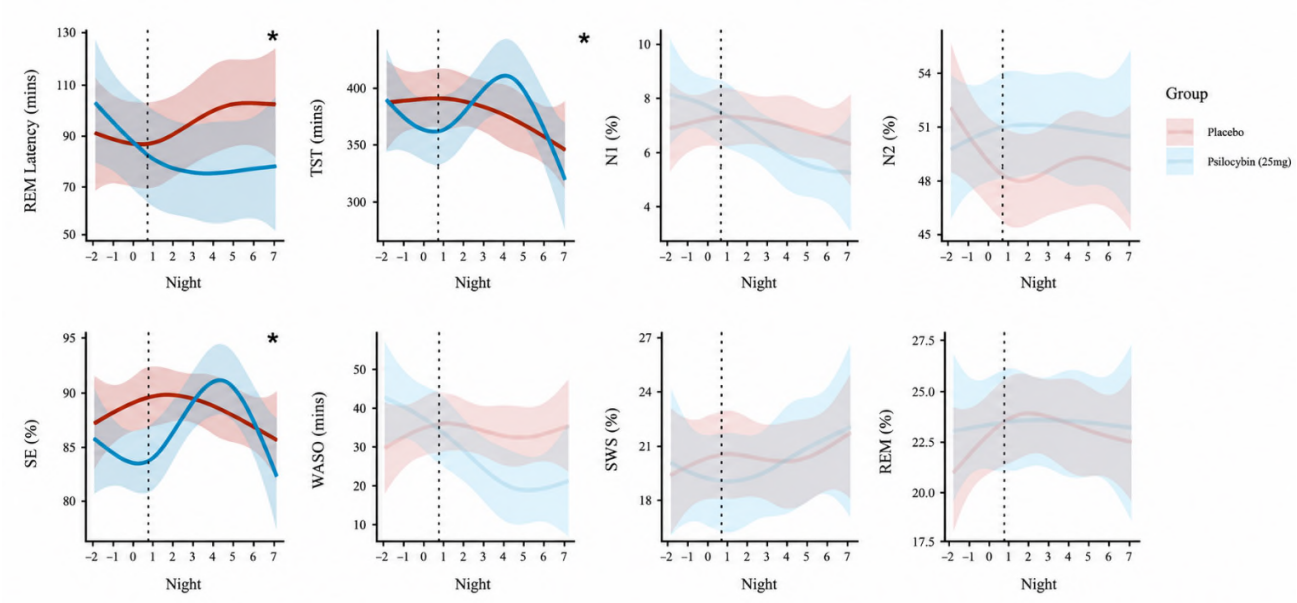


Fig. 4 Temporal trajectories of sleep architecture and continuity before and after psilocybin administration. Panels show model-predicted REM latency (minutes), total sleep time (TST; minutes), stage N1 and N2 sleep (%), sleep efficiency (SE; %), wake after sleep onset (WASO; minutes), slow-wave sleep (SWS; %), and REM sleep (%). Trajectories were estimated using linear mixed-effects models incorporating natural cubic splines for night (three degrees of freedom), treatment group, and their interactions, with participant-level random intercepts and adjustment for age, race, sex, baseline depressive symptom severity, and alcohol use. Blue lines represent psilocybin (25 mg) and red lines represent placebo; shaded bands indicate 95% confidence intervals. Nights −2 to 0 represent pre-treatment recordings, and nights +1 to +7 represent post-treatment recordings; vertical dotted lines mark dosing between nights 0 and +1. Nominal treatment-by-night interactions were observed for REM latency (p = .045), TST (p = .050), and SE (p = .015) for the first spline component, and WASO (p = .034) for the second spline component. Predicted TST and SE in the psilocybin group reached local maxima approximately four nights after dosing before declining, while REM latency decreased during the early post-treatment period.

Additional exploratory analyses

To investigate whether the temporal trajectories of sigma power and SWA were related, we conducted an exploratory analysis in which contemporaneous sigma power was included as a moderator of the non-linear relationship between study night and SWA. Sigma power significantly moderated the effects of all three natural spline basis functions describing the trajectory of SWA (basis 1: $p < 0.001$; basis 2: $p = 0.041$; basis 3: $p < 0.001$), suggesting that night-to-night changes in SWA varied as a function of sigma power. In those who received psilocybin, Pearson's correlation coefficients were calculated to understand whether changes in depressive symptoms (change score: baseline to +1 month after dosing session) or alcohol use (change score: baseline to +3 months after dosing session) were correlated with alterations in sleep, calculated by estimating the linear slope of change in spectral values over the seven nights post administration. None of the linear spectral slopes were significantly associated with change in percentage drinking days (all $|r| \leq .28$, all $p \geq .282$) or change in mean drinks per day (all $|r| \leq .43$, all $p \geq .147$). In contrast, change in GRID-HAMD score was significantly associated with the SWA slope, $r(12) = -.66$, $p = .011$, 95% CI [−.88, −.20] ($n = 14$), indicating that greater reductions in depressive symptoms were associated with greater reduction in SWA. GRID-HAMD change was not significantly associated with slopes in $delta_2$, theta, alpha, sigma, or beta power (all $|r| \leq .38$, all $p \geq .104$).

To assess the robustness of the primary findings to multiplicity across related sleep outcomes, supplementary analyses applied Benjamini–Hochberg false discovery rate (BH-FDR) correction across outcomes within each analysis domain, separately for each corresponding natural spline basis coefficient. For NREM spectral activity, the nominal treatment-by-night interactions observed for SWA and sigma power did not reach conventional significance thresholds following correction across the six NREM spectral outcomes (spline component 3: SWA = BH-FDR-adjusted $p = 0.096$; sigma = BH-FDR-adjusted $p = 0.096$ – see Table 3). No other NREM spectral treatment-by-night interaction was significant following BH-FDR correction. In contrast, the treatment-by-night effects observed for REM sigma and beta remained significant following correction across the four REM spectral outcomes. Specifically, the spline component 3 interaction remained significant for both REM sigma (BH-FDR-adjusted $p = 0.023$) and REM beta power (BH-FDR-adjusted $p = 0.013$ - Table 4). For sleep architecture, none of the nominal treatment-by-night effects remained significant following BH-FDR correction across the 11 architecture outcomes (all BH-FDR-adjusted $p > 0.05$ – Table 5). Collectively, these supplementary analyses indicated that the treatment-dependent REM sigma and beta trajectories were robust to correction for multiplicity across related outcomes, whereas the nominal NREM spectral and sleep-architecture effects were not. Similarly, sensitivity models demonstrating unadjusted models and models adjusted for the outcome values at baseline did not alter the interpretation of our findings (Tables S13-S18).

Functional analyses of NREM spectra

Function-on-scalar regression identified three discrete frequency intervals exhibiting significant between-group differences in the post-treatment NREM power spectra (Figure 5 - below). The psilocybin group exhibited significantly lower power within the 2.94–4.69 Hz and 11.3–14.1 Hz frequency ranges, relative to placebo. In contrast, psilocybin demonstrated significantly greater power within the 15.1–18.2 Hz range. Outside of these intervals, pointwise 95% confidence intervals for the estimated group effect overlapped zero, indicating no significant between-group differences. These findings suggest that when averaged across the post-drug period, spectral differences between groups were localized to the upper delta and sigma frequency ranges, rather than being uniformly distributed across the spectrum.

[Insert Figure 5 here, p18]

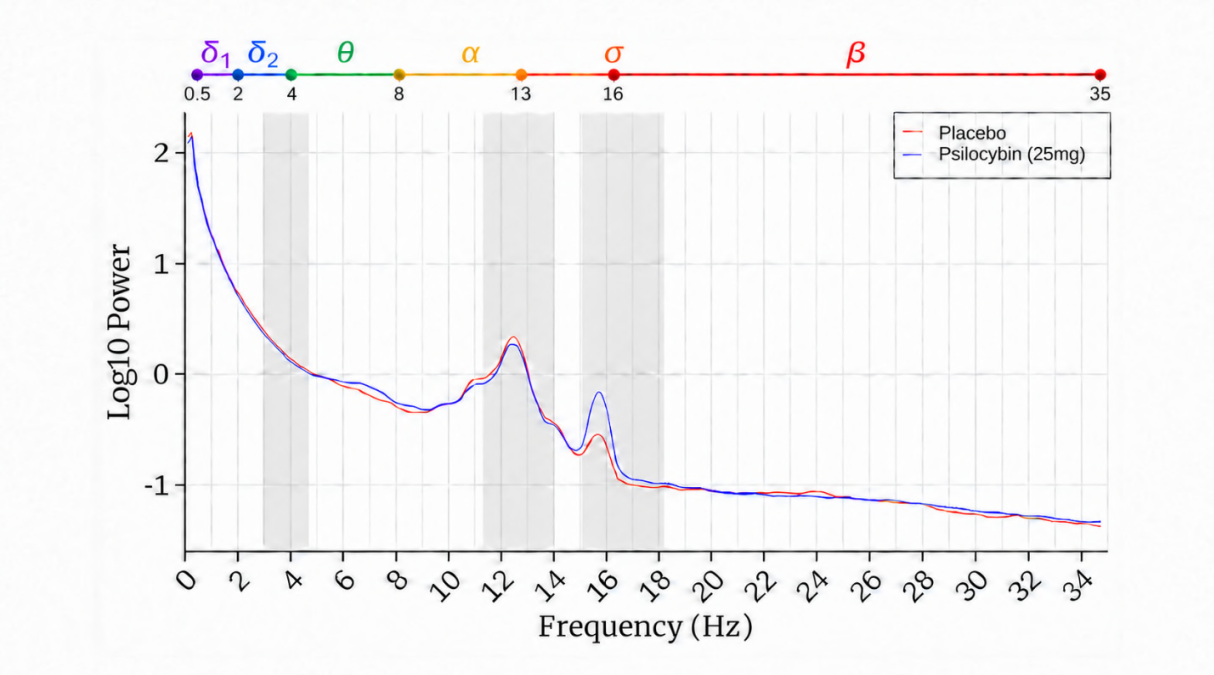


Fig. 5 NREM power spectra across the post-treatment recording period. Curves show log10-transformed spectral power during non-rapid eye movement (NREM) sleep, aggregated across nights +1 to +7 following administration of psilocybin (25 mg; blue) or placebo (red). The coloured bar above the plot indicates the frequency bands: slow-wave activity (SWA; δ_1, 0.5–2 Hz), delta2 (δ_2, 2–4 Hz), theta (θ, 4–8 Hz), alpha (α, 8–13 Hz), sigma (σ, 13–16 Hz), and beta (β, 16–35 Hz). Grey vertical shading identifies frequency intervals in which functional-on-scalar regression indicated between-group differences, defined by pointwise 95% confidence intervals for the treatment-group coefficient excluding zero. Confidence intervals were estimated using 2,000 participant-level bootstrap samples, resampled separately within treatment groups to preserve dependence among repeated nightly observations. Relative to placebo, the psilocybin group showed lower spectral power at 2.94–4.69 Hz and 11.3–14.1 Hz, and higher power at 15.1–18.2 Hz. These intervals represent pointwise evidence of differences and do not constitute simultaneous significance across the full spectrum

Discussion

In the present study, we examined the high-resolution temporal dynamics of sleep neurophysiology following psilocybin administration using longitudinal EEG recordings. The primary finding was that psilocybin-related effects on sleep were not expressed as acute changes, but instead emerged as nonlinear, time-dependent alterations in spectral dynamics across post-dosing nights, particularly within the oscillatory regimes of sigma and SWA, with consistent evidence that these trajectories differed between groups. In NREM sleep, group trajectory differences were most prominent in sigma and SWA, whilst in REM sleep, sigma and beta power showed analogous group-dependent temporal dynamics. Notably, these effects were driven by higher-order spline components, indicating that group differences were not static but instead reflected divergence in the shape of the temporal response.

Across both NREM and REM sleep, group differences in spectral power conformed to a curvilinear pattern, with effects peaking approximately two to four nights following drug administration before returning toward baseline. This delayed peak effect is consistent with emerging evidence suggesting that the neurophysiological effects of psychedelics may unfold over extended infradian timescales (Barrett, Doss et al. 2020, Doss, Považan et al. 2021, McCulloch, Madsen et al. 2022), potentially reflecting downstream processes such as synaptic plasticity or network reorganization (Ly, Greb et al. 2018, Nardou, Sawyer et al. 2023, Jiang, Shao et al. 2026), rather than immediate pharmacological action. This temporal profile is particularly notable given the absence of acute pre–post changes in both spectral bandpower and sleep architecture. Our time-restricted analyses comparing the night immediately before and after dosing revealed no significant effects across spectral or sleep continuity measures, with only limited evidence of interaction effects demonstrating increased REM duration and SE in the psilocybin group. The persistence of the REM spectral effects following correction for multiplicity provides the strongest statistical support for this delayed temporal profile, whereas the corresponding NREM effects should be interpreted more cautiously.

These findings provide greater texture to the only prior investigation of psilocybin's effects on sleep neurophysiology (Dudysová, Janků et al. 2020), in healthy adults (n=20), which reported prolonged REM latency and a trend towards shorter REM duration in the night immediately following psilocybin administration, as well as increased SWA in the first NREM cycle. Measured over the same timeframe, we observed a contrasting *increase* in REM duration (trend level) and no effects on SWA during the first NREM cycle (Table S12), although we did observe a trend-level *increase* in whole night SWA the night immediately following psilocybin administration. In similar contrast, when measured over an extended period of seven nights, we observed an overall *reduction* in REM latency. These contrasts may be due to our focus on a clinical, rather than healthy, population, and the extended and more ecologically valid timeframe over which they were assessed or may be explained in terms of a post-acute from homeostatic normalization of sleep following the acute pharmacological stimulus.

Together, these findings suggest that the primary impact of psilocybin on sleep is not immediate, but instead manifests through gradual, system-level changes in neural dynamics. Importantly, the absence of a fixed effect of condition (Psilocybin vs Placebo) for all spectral bands, suggests that these effects are not accounted for due to psilocybin generating a global shift in overall broadband or oscillatory specific power. Rather, the findings support a model in which psilocybin modulates the trajectory of sleep-related neural processes, with effects that evolve and dissipate across successive nights. The observation that linear sensitivity models failed to adequately capture the observed data, further serves to reinforce this interpretation.

Findings observed a high specificity within the frequency, as well as the temporal domain, with consistent modulation of SWA and sigma activity in NREM, and sigma and beta activity in REM, whilst other bands (e.g., delta[2], theta, alpha) showed little evidence of change. These patterns may reflect selective sensitivity of specific oscillatory systems to psilocybin-induced neuroplastic processes. Of note, NREM SWA and sigma displayed antiphasic and coupled temporal dynamics, where sigma elevation in the nights following drug administration was mirrored by a decline in SWA, with locally opposed maxima (*sigma*) and minima (*SWA*) occurring at night +3 within both powerbands (Figure 2). This bears potential significance as SWA and sigma activity are closely linked to synaptic homeostasis and thalamocortical function through their canonical transients, slow oscillations and sleep spindles, suggesting that psilocybin may preferentially modulate circuits involved in sleep-dependent plasticity, sensory gating, and memory consolidation (Schabus, Gruber et al. 2004, Wimmer, Astori et al. 2012, Fernandez and Lüthi 2020). Particularly within this context, slow oscillations and sleep spindles display well documented coupling behaviors (Yordanova, Kirov et al. 2017), suggesting the antiphasic changes we observed may be the result of a broader systems level change, rather than a selective and parallel augmentation of two discrete powerbands.

The presence of sigma-band effects across both NREM and REM sleep is also notable, as it may reflect broader modulation of thalamocortical gating mechanisms, which play a role in both sleep stability and sensory processing. Notably, psilocybin spectra averaged across post-administration nights (Figure 5) suggest overall sigma power elevations were narrowly localized to the 14–16 Hz range typically associated with fast-spindles (13–16 Hz) – transient oscillations known to subserve broad aspects of neurocognitive-functioning, neuroplasticity and sleep-dependent memory processes (Huupponen, Himanen et al. 2002, Andrillon, Nir et al. 2011, Mölle, Bergmann et al. 2011, Ujma, Konrad et al. 2014, Yordanova, Kirov et al. 2017). The absence of a similar increase within the slow-spindle band (8-13Hz), which preferentially mediate thalamocortical sensory-gating (Schabus, Gruber et al. 2004, Mölle, Bergmann et al. 2011, Schabus, Dang-Vu et al. 2012, Wimmer, Astori et al. 2012, Ngo, Martinetz et al. 2013, Dang-Vu, Hatch et al. 2017, Pereira, Beijamini et al. 2017), may reflect selective engagement of cognitive and mnemonic mechanisms. The scope of the present study did not extend to evaluating the functional consequences of spectral trajectories. As such, it remains unclear whether the observed effects have meaningful downstream functional implications. Moreover, as our signal processing framework did not extend to the explicit characterisation of sleep spindles, it remains possible that the sigma alterations could be a product of non-spindle aperiodic or $1/f$ signal origin. Future studies, appropriate in design and scope, are required to resolve these issues and determine functional significances.

In contrast to the robust effects observed in spectral power, sleep continuity and macro-architectural measures showed relatively limited changes. Whilst some group-dependent differences in trajectories were observed for SE, TST, and REM latency these effects were modest and again characterized by non-uniform divergence over time rather than consistent group differences. Notably, there was no evidence of systematic changes in sleep stage composition or global sleep structure. This dissociation suggests that psilocybin's effects on sleep may be more strongly expressed at the level of neural oscillations than at the level of gross sleep architecture. Such a pattern is consistent with the principle that spectral measures provide a more sensitive index of underlying neurophysiological processes, particularly in the context of interventions that produce general neuroplastic changes as opposed to sleep regulation *per se*.

Taken together, these findings support a model in which psilocybin exerts its effects on sleep through modulation of dynamic, state-dependent neural processes, rather than through direct or immediate alterations in sleep structure. The delayed and nonlinear nature of the observed effects are consistent with mechanisms involving plasticity-related changes in cortical and thalamocortical circuits, which may unfold over multiple days following drug administration. The absence of acute effects further argues against a simple pharmacological explanation and instead points toward secondary or downstream processes as the primary drivers of the observed changes. Speculatively, these may include alterations in synaptic strength, network connectivity, or homeostatic regulation of sleep, particularly within slow-wave and spindle generating systems.

Several limitations should be considered. The sample size, whilst greater than prior studies in this domain, limits the precision of effect estimates and the ability to detect smaller effects in secondary outcomes. Additionally, while spline-based modeling allowed for flexible characterization of temporal dynamics, the specific shape of these trajectories should be interpreted cautiously and replicated in larger samples. Second, although longitudinal at-home EEG enabled repeated assessment of sleep across multiple nights surrounding psilocybin administration, recordings were obtained using a limited frontal montage rather than full polysomnography or high-density EEG. Consequently, the present findings cannot establish the spatial distribution of the observed electrophysiological changes, and spectral sigma activity should not be interpreted as a direct measure of sleep spindle activity. Future work should aim to replicate these findings in larger, independent cohorts, examine the relationship between sleep-related changes and clinical or behavioral outcomes, and incorporate additional physiological measures (e.g., spindle characterization, aperiodic activity) to further elucidate mechanisms.

Overall, psilocybin was associated with delayed, nonlinear changes in sleep spectral dynamics, particularly within SWA and sigma frequency bands, with minimal evidence of acute effects on sleep architecture. These findings highlight the importance of longitudinal and nonlinear approaches in characterizing the neurophysiological effects of psychedelics and suggest that sleep may provide a sensitive window into the time-dependent processes underlying their therapeutic action.

Funding: This study was funded through extramural support from The Sleep Research Society, The Steven & Alexandra Cohen Foundation, and intramural funding from Johns Hopkins School of Medicine.

Conflicts of Interest: MJR is the patent holder for a wireless sleep-EEG system with intended use in precision medicine applications. FSB is a scientific advisor for and holds stock in MindState Design Labs, LLC, and is a scientific advisor for Mind Pharmaceuticals.

Contributions: M.J.R.: Conceptualization, Formal analysis, Investigation, Visualization, Writing – original draft, Writing – review & editing, Funding acquisition. E.W.: Investigation, Writing – review & editing. L.L.M.: Investigation, Visualization, Writing – review & editing. Z.Z.: Formal analysis, Investigation, Writing – review & editing. C.M.D.: Conceptualization, Formal analysis, Writing – review & editing. H.D.: Formal analysis, Visualization, Writing – review & editing. P.H.F.: Conceptualization, Supervision, Funding acquisition, Writing – review & editing. F.S.B.: Conceptualization, Investigation, Funding acquisition, Writing – review & editing. All authors reviewed and approved the final manuscript and agree to be accountable for the work.

Data availability: The data generated and/or analysed during the current study are not publicly available due to participant privacy and ethical considerations. Requests for access to de-identified data may be considered by the corresponding author and relevant institutional bodies, subject to applicable ethical, regulatory, and data-use requirements.

Code availability: The code used to perform the statistical analyses reported in this study is provided with the Supplementary Information and at the OSF page (https://osf.io/v4825). Additional code may be made available from the corresponding author upon reasonable request.

References

Andrillon, T., Y. Nir, R. J. Staba, F. Ferrarelli, C. Cirelli, G. Tononi and I. Fried (2011). "Sleep spindles in humans: insights from intracranial EEG and unit recordings." Journal of Neuroscience **31**(49): 17821-17834.

Arnedt, J. T., D. A. Conroy and K. J. Brower (2007). "Treatment options for sleep disturbances during alcohol recovery." Journal of addictive diseases **26**(4): 41-54.

Barrett, F. S., M. K. Doss, N. D. Sepeda, J. J. Pekar and R. R. Griffiths (2020). "Emotions and brain function are altered up to one month after a single high dose of psilocybin." Sci Rep **10**(1): 2214.

Bogenschutz, M. P., S. Ross, S. Bhatt, T. Baron, A. A. Forcehimes, E. Laska, S. E. Mennenga, K. O'Donnell, L. T. Owens and S. Podrebarac (2022). "Percentage of heavy drinking days following psilocybin-assisted psychotherapy vs placebo in the treatment of adult patients with alcohol use disorder: a randomized clinical trial." JAMA psychiatry **79**(10): 953-962.

Brower, K. J., M. S. Aldrich, E. A. Robinson, R. A. Zucker and J. F. Greden (2001). "Insomnia, self-medication, and relapse to alcoholism." American Journal of Psychiatry **158**(3): 399-404.

Brown, R. T., C. R. Nicholas, N. V. Cozzi, M. C. Gassman, K. M. Cooper, D. Muller, C. D. Thomas, S. J. Hetzel, K. M. Henriquez and A. S. Ribaudo (2017). "Pharmacokinetics of escalating doses of oral psilocybin in healthy adults." Clinical pharmacokinetics **56**(12): 1543-1554.

Carhart-Harris, R., B. Giribaldi, R. Watts, M. Baker-Jones, A. Murphy-Beiner, R. Murphy, J. Martell, A. Blemings, D. Erritzoe and D. J. Nutt (2021). "Trial of psilocybin versus escitalopram for depression." New England Journal of Medicine **384**(15): 1402-1411.

Chakravorty, S., N. S. Chaudhary and K. J. Brower (2016). "Alcohol dependence and its relationship with insomnia and other sleep disorders." Alcoholism: Clinical and Experimental Research **40**(11): 2271-2282.

Chaudhary, N. S., K. M. Kampman, H. R. Kranzler, M. A. Grandner, S. Debbarma and S. Chakravorty (2015). "Insomnia in alcohol dependent subjects is associated with greater psychosocial problem severity." Addictive behaviors **50**: 165-172.

Colrain, I. M., C. L. Nicholas and F. C. Baker (2014). "Alcohol and the sleeping brain." Handbook of clinical neurology **125**: 415-431.

Dang-Vu, T. T., B. Hatch, A. Salimi, M. Mograss, S. Boucetta, J. O'Byrne, M. Brandewinder, C. Berthomier and J. P. Gouin (2017). "Sleep spindles may predict response to cognitive-behavioral therapy for chronic insomnia." Sleep Med **39**: 54-61.

Davis, A. K., F. S. Barrett, D. G. May, M. P. Cosimano, N. D. Sepeda, M. W. Johnson, P. H. Finan and R. R. Griffiths (2021). "Effects of psilocybin-assisted therapy on major depressive disorder: a randomized clinical trial." JAMA psychiatry **78**(5): 481-489.
Dijk, D.-J., D. P. Brunner, D. G. Beersma and A. A. Borbély (1990). "Electroencephalogram power density and slow wave sleep as a function of prior waking and circadian phase." Sleep **13**(5): 430-440.
Doss, M. K., M. Považan, M. D. Rosenberg, N. D. Sepeda, A. K. Davis, P. H. Finan, G. S. Smith, J. J. Pekar, P. B. Barker and R. R. Griffiths (2021). "Psilocybin therapy increases cognitive and neural flexibility in patients with major depressive disorder." Translational psychiatry **11**(1): 1-10.
Dudysová, D., K. Janků, M. Šmotek, E. Saifutdinova, J. Kopřivová, J. Bušková, B. A. Mander, M. Brunovský, P. Zach and J. Korčák (2020). "The effects of daytime psilocybin administration on sleep: implications for antidepressant action." Frontiers in pharmacology **11**.
Edinger, J., R. Manber, A. Krystal and D. Buysse (2017). "0335 DOES OBJECTIVE SLEEP DURATION MODERATE TREATMENT RESPONSE IN PATIENT WITH COMORBID DEPRESSION AND INSOMNIA? A REPORT FROM THE TRIAD STUDY." Sleep **40**: A124.
Faul, F., E. Erdfelder, A. Buchner and A.-G. Lang (2009). "Statistical power analyses using G* Power 3.1: Tests for correlation and regression analyses." Behavior research methods **41**(4): 1149-1160.
Fernandez, L. M. and A. Lüthi (2020). "Sleep spindles: mechanisms and functions." Physiological reviews **100**(2): 805-868.
Finan, P. H., J. M. Richards, C. E. Gamaldo, D. Han, J. M. Leoutsakos, R. Salas, M. R. Irwin and M. T. Smith (2016). "Validation of a wireless, self-application, ambulatory electroencephalographic sleep monitoring device in healthy volunteers." Journal of Clinical Sleep Medicine **12**(11): 1443-1451.
Geoffroy, P. A., N. Hoertel, B. Etain, F. Bellivier, R. Delorme, F. Limosin and H. Peyre (2018). "Insomnia and hypersomnia in major depressive episode: prevalence, sociodemographic characteristics and psychiatric comorbidity in a population-based study." Journal of affective disorders **226**: 132-141.
Goldberg, S. B., B. T. Pace, C. R. Nicholas, C. L. Raison and P. R. Hutson (2020). "The experimental effects of psilocybin on symptoms of anxiety and depression: A meta-analysis." Psychiatry research **284**: 112749.
Hjorth, B. (1970). "EEG analysis based on time domain properties." Electroencephalography and clinical neurophysiology **29**(3): 306-310.
Hosein, M. M., M. J. Reid, S. Walser, S. Charney, G. A. Fonzo, B. R. Lewis, D. B. Yaden, T. Suppes, Z. A. Cordner and F. S. Barrett (2025). "Considerations and cautions for the integration of psilocybin into routine clinical care: a consensus statement from the US National Network of Depression Centers' Task Group on Psychedelics and Related Compounds." EClinicalMedicine **89**: 103517.
Huupponen, E., S.-L. Himanen, A. Värri, J. Hasan, M. Lehtokangas and J. Saarinen (2002). "A study on gender and age differences in sleep spindles." Neuropsychobiology **45**(2): 99-105.
Inada, K., M. Enomoto, K. Yamato, T. Marumoto, M. Takeshima and K. Mishima (2021). "Effect of residual insomnia and use of hypnotics on relapse of depression: a retrospective cohort study using a health insurance claims database." Journal of Affective Disorders **281**: 539-546.
Irwin, M., J. C. Gillin, J. Dang, J. Weissman, E. Phillips and C. L. Ehlers (2002). "Sleep deprivation as a probe of homeostatic sleep regulation in primary alcoholics." Biological psychiatry **51**(8): 632-641.
Jensen, M. E., D. S. Stenbæk, C. D. Messell, E. D. Poulsen, T. V. Varga, P. M. Fisher, M. K. K. Nielsen, S. S. Johansen, N. D. Volkow and G. M. Knudsen (2025). "Single-dose psilocybin therapy for alcohol use disorder: Pharmacokinetics, feasibility, safety and efficacy in an open-label study." Journal of Psychopharmacology **39**(5): 463-473.
Jiang, Q., L.-X. Shao, S. Yao, N. K. Savalia, A. D. Gilbert, P. A. Davoudian, J. D. Nothnagel, G. Tian, T. S. Hung, H. M. Lai, K. T. Beier, H. Zeng and A. C. Kwan (2026). "Psilocybin triggers an activity-dependent rewiring of large-scale cortical networks." Cell **189**(2): 659-675.e622.
Johnson, M. W., W. A. Richards and R. R. Griffiths (2008). "Human hallucinogen research: guidelines for safety." Journal of psychopharmacology **22**(6): 603-620.
Kolla, B. P., T. Schneekloth, J. Biernacka, M. Mansukhani, J. Geske, V. Karpyak, D. Hall-Flavin, L. Louikianova and M. A. Frye (2014). "The course of sleep disturbances in early alcohol recovery: an observational cohort study." The American journal on addictions **23**(1): 21-26.

Koob, G. F. and I. M. Colrain (2020). "Alcohol use disorder and sleep disturbances: a feed-forward allostatic framework." Neuropsychopharmacology **45**(1): 141-165.
Kupfer, D. J. and C. L. Ehlers (1989). "Two roads to rapid eye movement latency." Archives of general psychiatry **46**(10): 945-948.
Kupfer, D. J., E. Frank, A. B. McEachran and V. J. Grochocinski (1990). "Delta sleep ratio: a biological correlate of early recurrence in unipolar affective disorder." Archives of General Psychiatry **47**(12): 1100-1105.
Lechinger, J., J. Koch, S. L. Weinhold, M. Seeck-Hirschner, K. Stingele, C. Kropp-Näf, M. Braun, H. J. Drews, J. Aldenhoff and C. Huchzermeier (2021). "REM density is associated with treatment response in major depression: Antidepressant pharmacotherapy vs. psychotherapy." Journal of psychiatric research **133**: 67-72.
Levendowski, D. J., L. Ferini-Strambi, C. Gamaldo, M. Cetel, R. Rosenberg and P. R. Westbrook (2017). "The accuracy, night-to-night variability, and stability of frontopolar sleep electroencephalography biomarkers." Journal of Clinical Sleep Medicine **13**(6): 791-803.
Lotrich, F. E. and A. Germain (2015). "Decreased delta sleep ratio and elevated alpha power predict vulnerability to depression during interferon-alpha treatment." Acta neuropsychiatrica **27**(1): 14-24.
Ly, C., A. C. Greb, L. P. Cameron, J. M. Wong, E. V. Barragan, P. C. Wilson, K. F. Burbach, S. Soltanzadeh Zarandi, A. Sood, M. R. Paddy, W. C. Duim, M. Y. Dennis, A. K. McAllister, K. M. Ori-McKenney, J. A. Gray and D. E. Olson (2018). "Psychedelics Promote Structural and Functional Neural Plasticity." Cell Rep **23**(11): 3170-3182.
Manglick, M., S. M. Rajaratnam, J. Taffe, B. Tonge and G. Melvin (2013). "Persistent sleep disturbance is associated with treatment response in adolescents with depression." Australian & New Zealand Journal of Psychiatry **47**(6): 556-563.
Mariani, S., L. Tarokh, I. Djonlagic, B. E. Cade, M. G. Morrical, K. Yaffe, K. L. Stone, K. A. Loparo, S. M. Purcell and S. Redline (2018). "Evaluation of an automated pipeline for large-scale EEG spectral analysis: the National Sleep Research Resource." Sleep medicine **47**: 126-136.
McCulloch, D. E.-W., M. K. Madsen, D. S. Stenbaek, S. Kristiansen, B. Ozenne, P. S. Jensen, G. M. Knudsen and P. M. Fisher (2022). "Lasting effects of a single psilocybin dose on resting-state functional connectivity in healthy individuals." Journal of Psychopharmacology **36**(1): 74-84.
Miller, M. B., M. L. Donahue, K. B. Carey and L. A. J. Scott-Sheldon (2017). "Insomnia treatment in the context of alcohol use disorder: A systematic review and meta-analysis." Drug Alcohol Depend **181**: 200-207.
Mölle, M., T. O. Bergmann, L. Marshall and J. Born (2011). "Fast and slow spindles during the sleep slow oscillation: disparate coalescence and engagement in memory processing." Sleep **34**(10): 1411-1421.
Nardou, R., E. Sawyer, Y. J. Song, M. Wilkinson, Y. Padovan-Hernandez, J. L. de Deus, N. Wright, C. Lama, S. Faltin, L. A. Goff, G. L. Stein-O'Brien and G. Dölen (2023). "Psychedelics reopen the social reward learning critical period." Nature **618**(7966): 790-798.
Ngo, H. V., T. Martinetz, J. Born and M. Mölle (2013). "Auditory closed-loop stimulation of the sleep slow oscillation enhances memory." Neuron **78**(3): 545-553.
Nissen, C., B. Feige, A. König, U. Voderholzer, M. Berger and D. Riemann (2001). "Delta sleep ratio as a predictor of sleep deprivation response in major depression." Journal of psychiatric research **35**(3): 155-163.
Pereira, S. I. R., F. Beijamini, F. D. Weber, R. A. Vincenzi, F. A. C. da Silva and F. M. Louzada (2017). "Tactile stimulation during sleep alters slow oscillation and spindle densities but not motor skill." Physiology & behavior **169**: 59-68.
Pittenger, C. and R. S. Duman (2008). "Stress, depression, and neuroplasticity: a convergence of mechanisms." Neuropsychopharmacology **33**(1): 88-109.
Purcell, S., D. Manoach, C. Demanuele, B. Cade, S. Mariani, R. Cox, G. Panagiotaropoulou, R. Saxena, J. Pan and J. Smoller (2017). "Characterizing sleep spindles in 11,630 individuals from the National Sleep Research Resource." Nature communications **8**(1): 15930.

Reid, M. J., K. E. Dunn, L. Abraham, J. Ellis, C. Hunt, C. E. Gamaldo, W. G. Coon, C. J. Mun, E. C. Strain, M. T. Smith, P. H. Finan and A. S. Huhn (2024). "Suvorexant alters dynamics of the sleep-electroencephalography-power spectrum and depressive-symptom trajectories during inpatient opioid withdrawal." Sleep **47**(4).
Reid, M. J., H. Kettner, T. F. Blanken, B. Weiss and R. Carhartt-Harris (2024). "Preliminary evidence of sleep improvements following psilocybin administration, and their involvement in antidepressant therapeutic action." Current psychiatry reports **26**(11): 659-669.
Riemann, D., L. B. Krone, K. Wulff and C. Nissen (2020). "Sleep, insomnia, and depression." Neuropsychopharmacology **45**(1): 74-89.
Roberto, M. and F. P. Varodayan (2017). "Synaptic targets: Chronic alcohol actions." Neuropharmacology **122**: 85-99.
Roehrs, T. and T. Roth (2001). "Sleep, sleepiness, sleep disorders and alcohol use and abuse." Sleep medicine reviews **5**(4): 287-297.
Rush, A. J., M. H. Trivedi, H. M. Ibrahim, T. J. Carmody, B. Arnow, D. N. Klein, J. C. Markowitz, P. T. Ninan, S. Kornstein and R. Manber (2003). "The 16-Item Quick Inventory of Depressive Symptomatology (QIDS), clinician rating (QIDS-C), and self-report (QIDS-SR): a psychometric evaluation in patients with chronic major depression." Biological psychiatry **54**(5): 573-583.
Schabus, M., T. T. Dang-Vu, D. P. J. Heib, M. Boly, M. Desseilles, G. Vandewalle, C. Schmidt, G. Albouy, A. Darsaud and S. Gais (2012). "The fate of incoming stimuli during NREM sleep is determined by spindles and the phase of the slow oscillation." Frontiers in neurology **3**: 40.
Schabus, M., G. Gruber, S. Parapatics, C. Sauter, G. Klösch, P. Anderer, W. Klimesch, B. Saletu and J. Zeitlhofer (2004). "Sleep spindles and their significance for declarative memory consolidation." Sleep **27**(8): 1479-1485.
Stein, M. D. and P. D. Friedmann (2006). "Disturbed sleep and its relationship to alcohol use." Substance abuse **26**(1): 1-13.
Tamaki, M., H. Nittono, M. Hayashi and T. Hori (2005). "Examination of the first-night effect during the sleep-onset period." Sleep **28**(2): 195-202.
Troester MM., Q. S., Berry RB., et al., (2023). The AASM Manual for the Scoring of Sleep and Associated Events, Terminology and Technical Specifications. Version 3. . Darien, IL, American Academy of Sleep Medicine.
Troxel, W. M., D. J. Kupfer, C. F. Reynolds III, E. Frank, M. E. Thase, J. M. Miewald and D. J. Buysse (2011). "Insomnia and objectively measured sleep disturbances predict treatment outcome in depressed patients treated with psychotherapy or psychotherapy-pharmacotherapy combinations." The Journal of clinical psychiatry **72**(4): 9153.
Ujma, P. P., B. N. Konrad, L. Genzel, A. Bleifuss, P. Simor, A. Pótári, J. Körmendi, F. Gombos, A. Steiger and R. Bódizs (2014). "Sleep spindles and intelligence: evidence for a sexual dimorphism." Journal of Neuroscience **34**(49): 16358-16368.
Wei, L. J. and J. M. Lachin (1988). "Properties of the urn randomization in clinical trials." Control Clin Trials **9**(4): 345-364.
Wichniak, A., A. Wierzbicka and W. Jernajczyk (2013). "Sleep as a biomarker for depression." International review of psychiatry **25**(5): 632-645.
Williams, J. B., K. A. Kobak, P. Bech, N. Engelhardt, K. Evans, J. Lipsitz, J. Olin, J. Pearson and A. Kalali (2008). "The GRID-HAMD: standardization of the Hamilton depression rating scale." International clinical psychopharmacology **23**(3): 120-129.
Wimmer, R. D., S. Astori, C. T. Bond, Z. Rovó, J.-Y. Chatton, J. P. Adelman, P. Franken and A. Lüthi (2012). "Sustaining sleep spindles through enhanced SK2-channel activity consolidates sleep and elevates arousal threshold." Journal of Neuroscience **32**(40): 13917-13928.
Yordanova, J., R. Kirov, R. Verleger and V. Kolev (2017). "Dynamic coupling between slow waves and sleep spindles during slow wave sleep in humans is modulated by functional pre-sleep activation." Scientific Reports **7**(1): 14496.

Table 1: Baseline Demographics

	Placebo(N=18)	Psilocybin(N=22)	Overall(N=40)
Age at consent			
Mean (SD)	44.7 (10.7)	44.1 (11.3)	44.4 (10.9)
Median [Min, Max]	46.5 [23.0, 63.0]	45.0 [23.0, 61.0]	46.0 [23.0, 63.0]
Race			
Black/African American	1 (5.6%)	1 (4.5%)	2 (5.0%)
White/Caucasian	17 (94.4%)	20 (90.9%)	37 (92.5%)
Native American or Alaska Native	0 (0%)	1 (4.5%)	1 (2.5%)
Hispanic ethnicity			
No	18 (100%)	20 (90.9%)	38 (95.0%)
Yes	0 (0%)	2 (9.1%)	2 (5.0%)
Gender			
Female	7 (38.9%)	14 (63.6%)	21 (52.5%)
Male	11 (61.1%)	8 (36.4%)	19 (47.5%)
QIDS			
Mean (SD)	15.7 (4.17)	16.6 (3.79)	16.2 (3.94)
Median [Min, Max]	16.5 [9.00, 23.0]	16.0 [11.0, 23.0]	16.0 [9.00, 23.0]
PSQI global score, Prep1			
Mean (SD)	9.06 (3.25)	8.42 (2.59)	8.72 (2.89)
Median [Min, Max]	10.0 [4.00, 14.0]	8.00 [4.00, 14.0]	8.50 [4.00, 14.0]
Missing	1 (5.6%)	3 (13.6%)	4 (10.0%)
Baseline heavy drinking days			
Mean (SD)	35.3 (21.7)	32.4 (23.0)	33.7 (22.2)
Median [Min, Max]	38.5 [6.00, 77.0]	25.0 [6.00, 89.0]	25.5 [6.00, 89.0]
Baseline regular drinking days			
Mean (SD)	18.3 (19.9)	17.8 (19.9)	18.1 (19.6)
Median [Min, Max]	13.0 [0, 70.0]	13.5 [0, 71.0]	13.0 [0, 71.0]
Baseline abstinent days			
Mean (SD)	36.4 (23.9)	39.8 (21.7)	38.3 (22.5)
Median [Min, Max]	33.0 [2.00, 83.0]	44.5 [0, 75.0]	39.0 [0, 83.0]
Mean drinks per drinking day			
Mean (SD)	6.15 (3.38)	5.62 (2.06)	5.85 (2.69)

Median [Min, Max]	4.62 [2.49, 13.7]	4.96 [2.75, 10.3]	4.90 [2.49, 13.7]
Missing	1 (5.6%)	0 (0%)	1 (2.5%)
Mean drinks per heavy drinking day			
Mean (SD)	7.17 (2.73)	6.59 (2.01)	6.84 (2.33)
Median [Min, Max]	6.06 [4.78, 13.7]	5.96 [4.33, 11.5]	5.96 [4.33, 13.7]
Missing	1 (5.6%)	0 (0%)	1 (2.5%)
Maintained on antidepressant			
No	12 (66.7%)	13 (59.1%)	25 (62.5%)
Yes	6 (33.3%)	9 (40.9%)	15 (37.5%)
Baseline GRID-HAMD			
Mean (SD)	21.3 (4.73)	21.5 (4.72)	21.5 (4.66)
Median [Min, Max]	20.0 [15.0, 30.0]	21.0 [16.0, 37.0]	20.0 [15.0, 37.0]

SD, standard deviation; QIDS, Quick Inventory of Depressive Symptomatology; PSQI, Pittsburgh Sleep Quality Index; GRID-HAMD, GRID-Hamilton Depression Rating Scale.

Table 2: Sleep Variables at Baseline

	Placebo(N=18)	Psilocybin(N=22)	Overall(N=40)
TIB(mins)			
Mean (SD)	442 (90.3)	420 (121)	429 (109)
TST(mins)			
Mean (SD)	368 (118)	369 (114)	369 (116)
SE(%)			
Mean (SD)	83.3 (20.8)	87.1 (14.1)	85.5 (17.4)
SOL(mins)			
Mean (SD)	23.0 (28.7)	13.5 (15.3)	17.6 (22.6)
REM Latency			
Mean (SD)	83.5 (37.2)	91.4 (59.2)	88.0 (51.1)
Missing	7 (5.7%)	4 (2.5%)	11 (3.9%)
WASO(mins)			
Mean (SD)	31.8 (30.4)	31.7 (27.6)	31.8 (28.8)
N1(mins)			
Mean (SD)	23.5 (12.3)	25.8 (13.7)	24.8 (13.1)
N1(%)			
Mean (SD)	6.75 (4.67)	6.99 (3.17)	6.89 (3.88)
N2(mins)			
Mean (SD)	182 (68.8)	188 (70.7)	185 (69.8)
N2(%)			
Mean (SD)	49.1 (8.18)	50.4 (9.11)	49.8 (8.73)
N3(mins)			
Mean (SD)	72.4 (35.6)	69.5 (29.2)	70.7 (32.1)
N3(%)			
Mean (SD)	20.0 (9.07)	20.1 (9.76)	20.1 (9.45)
REM(mins)			
Mean (SD)	90.5 (37.5)	85.5 (38.5)	87.7 (38.1)
REM(%)			
Mean (SD)	24.1 (6.20)	22.5 (7.56)	23.2 (7.04)
Arousals(#)			
Mean (SD)	73.5 (34.0)	76.2 (46.4)	75.0 (41.4)
REM Periods(#)			
Mean (SD)	4.64 (2.08)	4.69 (2.28)	4.67 (2.19)

SWS Periods(#)			
Mean (SD)	3.80 (1.93)	4.28 (2.18)	4.07 (2.09)
NREM Arousal Index(#/min)			
Mean (SD)	16.5 (7.16)	16.0 (7.56)	16.2 (7.38)
REM Arousal Index(#/min)			
Mean (SD)	16.1 (8.82)	12.8 (8.03)	14.2 (8.52)

SD, standard deviation; TIB, time in bed; TST, total sleep time; SE, sleep efficiency; SOL, sleep onset latency; WASO, wake after sleep onset; N1/N2/N3, NREM sleep stages 1-3; REM, rapid eye movement sleep; SWS, slow-wave sleep.

Table 3: NREM Spline Models

Outcome	Term	Estimate	SE	df	t	p	95% CI lower	95% CI upper	REML	AIC
SWA [0.5-2Hz]	(Intercept)	102.724	9.727	42.075	10.561	0.000	83.096	122.352	1909.033	1939.033
	age	-0.168	0.099	35.847	-1.704	0.097	-0.368	0.032	1909.033	1939.033
	race	-0.303	2.139	33.446	-0.142	0.888	-4.652	4.046	1909.033	1939.033
	sex	-0.015	2.131	33.647	-0.007	0.994	-4.349	4.318	1909.033	1939.033
	QIDS	-0.258	0.286	33.362	-0.905	0.372	-0.839	0.322	1909.033	1939.033
	TLFB	-0.062	0.047	33.161	-1.303	0.201	-0.159	0.035	1909.033	1939.033
	Night Spline Component #1	-4.085	4.914	249.707	-0.831	0.407	-13.764	5.593	1909.033	1939.033
	Night Spline Component #2	-14.488	8.528	250.050	-1.699	0.091	-31.284	2.309	1909.033	1939.033
	Night Spline Component #3	-8.015	3.799	249.351	-2.110	0.036	-15.498	-0.533	1909.033	1939.033
	group	-5.267	2.938	117.427	-1.793	0.076	-11.085	0.550	1909.033	1939.033
	Night Spline Component #1:group	1.330	3.251	252.685	0.409	0.683	-5.071	7.732	1909.033	1939.033
	Night Spline Component #2:group	9.883	5.614	251.199	1.761	0.080	-1.173	20.939	1909.033	1939.033
	Night Spline Component #3:group	5.481	2.541	250.756	2.157	0.032	0.477	10.485	1909.033	1939.033
Delta$_2$ [2-4Hz]	(Intercept)	7.742	2.521	37.612	3.071	0.004	2.636	12.848	1099.838	1129.838
	age	0.049	0.026	33.506	1.881	0.069	-0.004	0.101	1099.838	1129.838
	race	0.499	0.563	31.767	0.886	0.382	-0.648	1.646	1099.838	1129.838
	sex	-0.662	0.561	31.883	-1.181	0.246	-1.805	0.480	1099.838	1129.838
	QIDS	0.068	0.075	31.653	0.898	0.376	-0.086	0.221	1099.838	1129.838
	TLFB	0.007	0.013	31.505	0.540	0.593	-0.019	0.032	1099.838	1129.838
	Night Spline Component #1	0.387	1.104	245.961	0.351	0.726	-1.786	2.561	1099.838	1129.838
	Night Spline Component #2	-1.094	1.915	246.244	-0.571	0.568	-4.867	2.678	1099.838	1129.838
	Night Spline Component #3	-0.397	0.853	245.548	-0.465	0.642	-2.077	1.283	1099.838	1129.838
	group	-0.458	0.718	90.317	-0.638	0.525	-1.884	0.967	1099.838	1129.838
	Night Spline Component #1:group	-0.297	0.731	248.489	-0.406	0.685	-1.736	1.142	1099.838	1129.838
	Night Spline Component #2:group	1.165	1.261	247.195	0.923	0.357	-1.320	3.649	1099.838	1129.838
	Night Spline Component #3:group	0.170	0.571	246.702	0.297	0.767	-0.955	1.294	1099.838	1129.838
Theta [4-8 Hz]	(Intercept)	1.078	1.293	36.172	0.834	0.410	-1.544	3.700	551.856	581.856
	age	0.024	0.013	34.422	1.773	0.085	-0.003	0.051	551.856	581.856
	race	0.343	0.295	33.560	1.163	0.253	-0.257	0.944	551.856	581.856
	sex	0.085	0.294	33.583	0.289	0.774	-0.513	0.683	551.856	581.856
	QIDS	0.009	0.039	33.450	0.232	0.818	-0.071	0.089	551.856	581.856
	TLFB	-0.001	0.007	33.375	-0.117	0.907	-0.014	0.013	551.856	581.856
	Night Spline Component #1	0.041	0.388	243.466	0.105	0.917	-0.724	0.805	551.856	581.856

	Night Spline Component #2	0.017	0.674	243.610	0.025	0.980	-1.310	1.344	551.856	581.856
	Night Spline Component #3	-0.218	0.300	243.184	-0.726	0.468	-0.808	0.373	551.856	581.856
	group	0.154	0.329	59.004	0.469	0.641	-0.504	0.812	551.856	581.856
	Night Spline Component #1:group	0.003	0.257	244.724	0.012	0.991	-0.504	0.510	551.856	581.856
	Night Spline Component #2:group	0.121	0.444	244.059	0.274	0.785	-0.753	0.996	551.856	581.856
	Night Spline Component #3:group	0.197	0.201	243.728	0.983	0.327	-0.198	0.593	551.856	581.856
Alpha [8-13Hz]	(Intercept)	-5.795	3.867	34.757	-1.498	0.143	-13.649	2.058	1163.080	1193.080
	age	0.085	0.040	32.984	2.124	0.041	0.004	0.167	1163.080	1193.080
	race	-0.369	0.883	32.116	-0.418	0.679	-2.166	1.429	1163.080	1193.080
	sex	1.262	0.879	32.141	1.436	0.161	-0.528	3.052	1163.080	1193.080
	QIDS	0.156	0.118	32.007	1.326	0.194	-0.084	0.397	1163.080	1193.080
	TLFB	-0.008	0.020	31.932	-0.394	0.697	-0.048	0.032	1163.080	1193.080
	Night Spline Component #1	1.236	1.187	242.261	1.042	0.299	-1.101	3.574	1163.080	1193.080
	Night Spline Component #2	3.264	2.060	242.417	1.584	0.114	-0.795	7.322	1163.080	1193.080
	Night Spline Component #3	-0.768	0.917	241.959	-0.838	0.403	-2.575	1.039	1163.080	1193.080
	group	1.389	0.988	58.002	1.405	0.165	-0.590	3.367	1163.080	1193.080
	Night Spline Component #1:group	-0.491	0.787	243.624	-0.624	0.533	-2.042	1.059	1163.080	1193.080
	Night Spline Component #2:group	-1.992	1.358	242.905	-1.467	0.144	-4.666	0.682	1163.080	1193.080
	Night Spline Component #3:group	0.707	0.614	242.550	1.152	0.251	-0.502	1.917	1163.080	1193.080
Sigma [13-16 Hz]	(Intercept)	-5.381	8.119	52.600	-0.663	0.510	-21.669	10.907	1910.437	1940.437
	age	0.008	0.080	40.560	0.102	0.919	-0.154	0.171	1910.437	1940.437
	race	-0.204	1.726	36.753	-0.118	0.907	-3.701	3.293	1910.437	1940.437
	sex	-0.646	1.722	37.143	-0.375	0.710	-4.133	2.842	1910.437	1940.437
	QIDS	0.018	0.230	36.779	0.076	0.940	-0.449	0.484	1910.437	1940.437
	TLFB	0.061	0.038	36.477	1.592	0.120	-0.017	0.139	1910.437	1940.437
	Night Spline Component #1	1.691	5.047	255.823	0.335	0.738	-8.248	11.629	1910.437	1940.437
	Night Spline Component #2	11.126	8.756	256.280	1.271	0.205	-6.117	28.370	1910.437	1940.437
	Night Spline Component #3	8.621	3.902	255.784	2.209	0.028	0.936	16.305	1910.437	1940.437
	group	3.903	2.719	170.697	1.435	0.153	-1.465	9.271	1910.437	1940.437
	Night Spline Component #1:group	0.062	3.331	259.266	0.019	0.985	-6.498	6.623	1910.437	1940.437
	Night Spline Component #2:group	-8.216	5.759	257.663	-1.427	0.155	-19.557	3.125	1910.437	1940.437
	Night Spline Component #3:group	-5.880	2.607	257.517	-2.255	0.025	-11.014	-0.745	1910.437	1940.437
Beta [16-35 Hz]	(Intercept)	-0.786	0.497	47.750	-1.583	0.120	-1.785	0.213	346.744	376.744
	age	0.006	0.005	38.231	1.124	0.268	-0.004	0.016	346.744	376.744
	race	-0.030	0.107	34.990	-0.283	0.779	-0.247	0.187	346.744	376.744
	sex	0.019	0.107	35.309	0.177	0.860	-0.198	0.235	346.744	376.744
	QIDS	0.021	0.014	34.973	1.486	0.146	-0.008	0.050	346.744	376.744

	TLFB	0.004	0.002	34.710	1.887	0.068	0.000	0.009	346.744	376.744
	Night Spline Component #1	0.192	0.289	253.431	0.664	0.507	-0.377	0.760	346.744	376.744
	Night Spline Component #2	0.539	0.501	253.852	1.077	0.283	-0.447	1.526	346.744	376.744
	Night Spline Component #3	0.196	0.223	253.246	0.878	0.381	-0.244	0.635	346.744	376.744
	group	0.241	0.161	150.720	1.503	0.135	-0.076	0.558	346.744	376.744
	Night Spline Component #1:group	-0.130	0.191	256.817	-0.681	0.496	-0.505	0.246	346.744	376.744
	Night Spline Component #2:group	-0.400	0.330	255.195	-1.214	0.226	-1.049	0.249	346.744	376.744
	Night Spline Component #3:group	-0.173	0.149	254.911	-1.161	0.247	-0.467	0.121	346.744	376.744

SE, standard error; df, degrees of freedom (Satterthwaite approximation); t, t value; p, p value ($p < 0.001$ replaces very small or source-rounded zero values); REML, restricted maximum likelihood criterion; AIC, Akaike information criterion; Night Spline Component #, natural cubic spline basis for night; group, treatment group (psilocybin vs. placebo); QIDS, baseline QIDS-SR score; TLFB, Timeline Followback; rel_SWA/rel_delta2/rel_delta/Theta [4-8 Hz]/Alpha [8-13 Hz]/Sigma [13-16 Hz]/Beta [16-35 Hz], relative EEG spectral power (%) in the corresponding frequency band (see Table S1).

Table 4: REM Spline Models

Outcome	Term	Estimate	Std. Error	df	t value	Pr(>|t|)	95% CI Low	95% CI High	REML	AIC
Theta [4-8 Hz]	(Intercept)	3.504	1.114	39.370	3.146	0.003	1.251	5.756	633.695	663.695
	age	-0.004	0.011	34.751	-0.381	0.706	-0.028	0.019	633.695	663.695
	race	0.189	0.248	32.562	0.762	0.452	-0.316	0.695	633.695	663.695
	sex	-0.530	0.248	32.573	-2.138	0.040	-1.035	-0.026	633.695	663.695
	QIDS	-0.023	0.033	32.348	-0.699	0.490	-0.090	0.044	633.695	663.695
	TLFB	0.001	0.006	32.387	0.204	0.840	-0.010	0.012	633.695	663.695
	Night Spline Component #1	-0.539	0.537	229.006	-1.004	0.316	-1.597	0.519	633.695	663.695
	Night Spline Component #2	-0.460	0.935	229.090	-0.492	0.623	-2.302	1.382	633.695	663.695
	Night Spline Component #3	-0.737	0.418	228.395	-1.761	0.080	-1.561	0.088	633.695	663.695
	group	-0.150	0.333	104.182	-0.450	0.654	-0.811	0.511	633.695	663.695
	Night Spline Component #1:group	0.348	0.359	231.660	0.971	0.333	-0.359	1.056	633.695	663.695
	Night Spline Component #2:group	0.266	0.620	230.183	0.429	0.669	-0.955	1.486	633.695	663.695
	Night Spline Component #3:group	0.547	0.286	229.699	1.909	0.057	-0.017	1.111	633.695	663.695
Alpha [8-13 Hz]	(Intercept).	-1.239	4.688	33.638	-0.264	0.793	-10.770	8.291	1270.760	1300.760
	age	0.067	0.049	31.123	1.384	0.176	-0.032	0.166	1270.760	1300.760
	race	-0.311	1.063	29.894	-0.293	0.772	-2.481	1.860	1270.760	1300.760
	sex	-0.693	1.061	29.695	-0.652	0.519	-2.861	1.476	1270.760	1300.760
	QIDS	0.090	0.141	29.529	0.635	0.531	-0.199	0.379	1270.760	1300.760
	TLFB	-0.011	0.024	29.612	-0.462	0.647	-0.059	0.037	1270.760	1300.760
	Night Spline Component #1	0.633	1.844	223.610	0.343	0.732	-3.002	4.268	1270.760	1300.760
	Night Spline Component #2	2.567	3.211	223.555	0.799	0.425	-3.761	8.895	1270.760	1300.760
	Night Spline Component #3	-1.875	1.436	222.893	-1.305	0.193	-4.705	0.956	1270.760	1300.760
	group	1.372	1.299	72.322	1.056	0.294	-1.217	3.960	1270.760	1300.760
	Night Spline Component #1:group	-0.803	1.234	225.686	-0.650	0.516	-3.235	1.630	1270.760	1300.760
	Night Spline Component #2:group	-2.002	2.129	224.402	-0.940	0.348	-6.197	2.194	1270.760	1300.760
	Night Spline Component #3:group	1.180	0.984	223.866	1.200	0.232	-0.759	3.119	1270.760	1300.760
Sigma [13-16 Hz]	(Intercept)	1.582	7.906	50.927	0.200	0.842	-14.289	17.454	1747.808	1777.808
	age	0.004	0.079	39.927	0.057	0.955	-0.155	0.164	1747.808	1777.808
	race	-0.190	1.691	35.519	-0.112	0.911	-3.622	3.242	1747.808	1777.808
	sex	-1.575	1.692	36.258	-0.931	0.358	-5.004	1.855	1747.808	1777.808
	QIDS	-0.103	0.225	35.995	-0.459	0.649	-0.559	0.353	1747.808	1777.808

	TLFB	0.059	0.038	35.849	1.565	0.126	-0.017	0.135	1747.808	1777.808
	Night Spline Component #1	-1.441	5.018	236.157	-0.287	0.774	-11.327	8.444	1747.808	1777.808
	Night Spline Component #2	1.966	8.734	236.613	0.225	0.822	-15.241	19.173	1747.808	1777.808
	Night Spline Component #3	9.806	3.911	236.196	2.507	0.013	2.102	17.510	1747.808	1777.808
	group	0.641	2.710	165.427	0.237	0.813	-4.709	5.992	1747.808	1777.808
	Night Spline Component #1:group	2.445	3.345	239.497	0.731	0.466	-4.144	9.034	1747.808	1777.808
	Night Spline Component #2:group	0.449	5.781	238.006	0.078	0.938	-10.940	11.838	1747.808	1777.808
	Night Spline Component #3:group	-6.819	2.673	238.012	-2.551	0.011	-12.085	-1.553	1747.808	1777.808
Beta [16-35 Hz]	(Intercept)	0.120	0.377	40.922	0.318	0.752	-0.642	0.882	122.785	152.785
	age	0.001	0.004	35.119	0.384	0.703	-0.006	0.009	122.785	152.785
	race	0.022	0.083	32.459	0.258	0.798	-0.148	0.191	122.785	152.785
	sex	-0.175	0.083	32.625	-2.107	0.043	-0.345	-0.006	122.785	152.785
	QIDS	0.000	0.011	32.386	0.039	0.969	-0.022	0.023	122.785	152.785
	TLFB	0.004	0.002	32.386	2.091	0.044	0.000	0.008	122.785	152.785
	Night Spline Component #1	-0.125	0.198	230.407	-0.630	0.529	-0.514	0.265	122.785	152.785
	Night Spline Component #2	0.143	0.344	230.584	0.415	0.678	-0.535	0.821	122.785	152.785
	Night Spline Component #3	0.479	0.154	229.898	3.111	0.002	0.176	0.782	122.785	152.785
	group	0.105	0.117	118.414	0.894	0.373	-0.127	0.337	122.785	152.785
	Night Spline Component #1:group	0.113	0.132	233.390	0.854	0.394	-0.147	0.373	122.785	152.785
	Night Spline Component #2:group	-0.022	0.228	231.818	-0.097	0.923	-0.471	0.427	122.785	152.785
	Night Spline Component #3:group	-0.315	0.105	231.400	-2.986	0.003	-0.522	-0.107	122.785	152.785

Table 5: Sleep Architecture Spline Models.

outcome	term	Estimate	Std. Error	df	t value	Pr(>|t|)	95% CI Low	95% CI High	REML	AIC
Sleep Efficiency (%)	(Intercept)	90.406	10.203	60.234	8.861	0.000	69.999	110.814	2101.864	2131.864
	age	-0.172	0.094	34.169	-1.821	0.077	-0.363	0.020	2101.864	2131.864
	race	0.525	1.975	29.415	0.266	0.792	-3.513	4.562	2101.864	2131.864
	Sex	-1.682	1.994	29.880	-0.844	0.406	-5.754	2.391	2101.864	2131.864
	QIDS	0.222	0.264	29.486	0.840	0.408	-0.318	0.761	2101.864	2131.864
	TLFB	0.115	0.044	29.064	2.620	0.014	0.025	0.204	2101.864	2131.864
	Night Spline Component #1	-13.208	8.459	251.438	-1.561	0.120	-29.867	3.452	2101.864	2131.864
	Night Spline Component #2	7.948	14.728	252.724	0.540	0.590	-21.058	36.953	2101.864	2131.864
	Night Spline Component #3	-5.617	6.581	253.292	-0.853	0.394	-18.577	7.344	2101.864	2131.864
	group	-2.774	4.148	222.723	-0.669	0.504	-10.949	5.400	2101.864	2131.864
	Night Spline Component #1:group	13.758	5.614	256.094	2.451	0.015	2.703	24.813	2101.864	2131.864
	Night Spline Component #2:group	-5.955	9.817	255.218	-0.607	0.545	-25.288	13.379	2101.864	2131.864
	Night Spline Component #3:group	1.750	4.463	256.318	0.392	0.695	-7.039	10.539	2101.864	2131.864
TST (mins)	(Intercept)	372.711	114.780	40.608	3.247	0.002	140.840	604.583	3198.624	3228.624
	age	0.059	1.153	33.018	0.051	0.960	-2.287	2.404	3198.624	3228.624
	race	-20.985	24.878	30.389	-0.844	0.406	-71.766	29.795	3198.624	3228.624
	Sex	3.235	25.007	30.708	0.129	0.898	-47.787	54.258	3198.624	3228.624
	QIDS	-1.573	3.323	30.370	-0.473	0.639	-8.356	5.210	3198.624	3228.624
	TLFB	1.020	0.552	30.131	1.848	0.074	-0.107	2.148	3198.624	3228.624
	Night Spline Component #1	-95.194	64.055	242.138	-1.486	0.139	-221.370	30.983	3198.624	3228.624
	Night Spline Component #2	42.420	111.657	242.646	0.380	0.704	-177.522	262.361	3198.624	3228.624
	Night Spline Component #3	-51.202	49.875	241.931	-1.027	0.306	-149.448	47.043	3198.624	3228.624
	group	2.235	36.884	130.538	0.061	0.952	-70.733	75.202	3198.624	3228.624
	Night Spline Component #1:group	84.168	42.780	245.931	1.967	0.050	-0.095	168.431	3198.624	3228.624
	Night Spline Component #2:group	-62.488	74.674	244.573	-0.837	0.404	-209.573	84.597	3198.624	3228.624
	Night Spline Component #3:group	3.994	33.958	244.077	0.118	0.906	-62.894	70.882	3198.624	3228.624
WASO (mins)	(Intercept)	-7.482	25.460	54.735	-0.294	0.770	-58.511	43.548	2536.349	2566.349
	age	0.742	0.243	35.833	3.050	0.004	0.248	1.235	2536.349	2566.349
	race	3.372	5.148	31.423	0.655	0.517	-7.121	13.866	2536.349	2566.349
	Sex	-0.604	5.189	31.993	-0.116	0.908	-11.173	9.965	2536.349	2566.349
	QIDS	-0.551	0.688	31.566	-0.800	0.430	-1.952	0.851	2536.349	2566.349

	TLFB	-0.232	0.114	31.188	-2.030	0.051	-0.464	0.001	2536.349	2566.349
	Night Spline Component #1	21.956	18.974	249.685	1.157	0.248	-15.413	59.326	2536.349	2566.349
	Night Spline Component #2	58.128	33.053	250.612	1.759	0.080	-6.968	123.225	2536.349	2566.349
	Night Spline Component #3	16.848	14.770	250.574	1.141	0.255	-12.241	45.938	2536.349	2566.349
	group	20.745	9.650	202.481	2.150	0.033	1.717	39.773	2536.349	2566.349
	Night Spline Component #1:group	-24.464	12.619	254.146	-1.939	0.054	-49.316	0.388	2536.349	2566.349
	Night Spline Component #2:group	-47.028	22.057	252.983	-2.132	0.034	-90.467	-3.589	2536.349	2566.349
	Night Spline Component #3:group	-17.433	10.032	253.368	-1.738	0.083	-37.189	2.323	2536.349	2566.349
SOL (mins)	(Intercept)	-7.442	23.917	42.109	-0.311	0.757	-55.704	40.820	2414.015	2444.015
	age	-0.010	0.237	32.291	-0.042	0.967	-0.493	0.473	2414.015	2444.015
	race	-2.699	5.090	29.243	-0.530	0.600	-13.106	7.708	2414.015	2444.015
	Sex	6.667	5.120	29.643	1.302	0.203	-3.796	17.129	2414.015	2444.015
	QIDS	0.471	0.680	29.281	0.692	0.494	-0.919	1.861	2414.015	2444.015
	TLFB	-0.087	0.113	29.010	-0.766	0.450	-0.318	0.144	2414.015	2444.015
	Night Spline Component #1	-0.651	14.743	243.534	-0.044	0.965	-29.692	28.389	2414.015	2444.015
	Night Spline Component #2	-0.454	25.695	244.181	-0.018	0.986	-51.067	50.159	2414.015	2444.015
	Night Spline Component #3	12.847	11.480	243.554	1.119	0.264	-9.766	35.459	2414.015	2444.015
	group	10.855	8.099	150.701	1.340	0.182	-5.146	26.857	2414.015	2444.015
	Night Spline Component #1:group	-4.933	9.835	247.885	-0.502	0.616	-24.304	14.438	2414.015	2444.015
	Night Spline Component #2:group	2.287	17.174	246.427	0.133	0.894	-31.539	36.114	2414.015	2444.015
	Night Spline Component #3:group	-12.037	7.811	246.093	-1.541	0.125	-27.422	3.347	2414.015	2444.015
REM latency (mins)	(Intercept)	-15.972	58.309	39.404	-0.274	0.786	-133.875	101.931	2702.203	2732.203
	age	0.640	0.596	34.566	1.075	0.290	-0.570	1.849	2702.203	2732.203
	race	-9.808	12.942	32.541	-0.758	0.454	-36.151	16.536	2702.203	2732.203
	Sex	3.184	13.008	32.839	0.245	0.808	-23.285	29.654	2702.203	2732.203
	QIDS	2.078	1.730	32.495	1.201	0.238	-1.443	5.598	2702.203	2732.203
	TLFB	0.604	0.288	32.498	2.097	0.044	0.018	1.191	2702.203	2732.203
	Night Spline Component #1	52.499	27.387	235.904	1.917	0.056	-1.455	106.453	2702.203	2732.203
	Night Spline Component #2	58.452	47.282	235.652	1.236	0.218	-34.697	151.602	2702.203	2732.203
	Night Spline Component #3	42.028	21.313	235.215	1.972	0.050	0.040	84.016	2702.203	2732.203
	group	18.075	17.240	101.312	1.048	0.297	-16.123	52.272	2702.203	2732.203
	Night Spline Component #1:group	-37.047	18.418	238.885	-2.011	0.045	-73.330	-0.764	2702.203	2732.203
	Night Spline Component #2:group	-54.784	31.648	236.884	-1.731	0.085	-117.131	7.563	2702.203	2732.203
	Night Spline Component #3:group	-25.931	14.670	236.459	-1.768	0.078	-54.831	2.970	2702.203	2732.203
N1 (%)	(Intercept)	1.837	2.946	75.514	0.624	0.535	-4.032	7.706	1507.529	1537.529
	age	0.061	0.025	32.300	2.392	0.023	0.009	0.112	1507.529	1537.529

	race	0.048	0.522	27.514	0.092	0.927	-1.023	1.119	1507.529	1537.529
	sex	0.216	0.529	27.395	0.409	0.686	-0.868	1.300	1507.529	1537.529
	QIDS	0.084	0.070	26.931	1.198	0.241	-0.060	0.227	1507.529	1537.529
	TLFB	-0.019	0.012	26.132	-1.687	0.103	-0.043	0.004	1507.529	1537.529
	Night Spline Component #1	2.867	2.839	253.786	1.010	0.314	-2.725	8.458	1507.529	1537.529
	Night Spline Component #2	3.750	4.933	255.201	0.760	0.448	-5.964	13.464	1507.529	1537.529
	Night Spline Component #3	0.984	2.218	257.232	0.444	0.658	-3.384	5.352	1507.529	1537.529
	group	1.660	1.329	244.053	1.249	0.213	-0.958	4.279	1507.529	1537.529
	Night Spline Component #1:group	-2.937	1.883	258.269	-1.560	0.120	-6.644	0.770	1507.529	1537.529
	Night Spline Component #2:group	-3.800	3.288	257.118	-1.156	0.249	-10.274	2.674	1507.529	1537.529
	Night Spline Component #3:group	-1.973	1.517	259.691	-1.301	0.194	-4.959	1.013	1507.529	1537.529
N2 (%)	(Intercept)	38.143	9.946	40.687	3.835	0.000	18.053	58.233	1858.690	1888.690
	age	0.213	0.101	34.341	2.118	0.041	0.009	0.418	1858.690	1888.690
	race	-0.208	2.181	31.985	-0.096	0.924	-4.651	4.234	1858.690	1888.690
	sex	-1.210	2.192	32.304	-0.552	0.585	-5.674	3.254	1858.690	1888.690
	QIDS	0.550	0.291	31.965	1.887	0.068	-0.044	1.143	1858.690	1888.690
	TLFB	0.080	0.048	31.683	1.647	0.109	-0.019	0.178	1858.690	1888.690
	Night Spline Component #1	-2.013	5.147	240.964	-0.391	0.696	-12.152	8.125	1858.690	1888.690
	Night Spline Component #2	-19.128	8.954	241.070	-2.136	0.034	-36.766	-1.489	1858.690	1888.690
	Night Spline Component #3	-1.027	4.029	240.287	-0.255	0.799	-8.963	6.909	1858.690	1888.690
	group	-5.237	3.077	118.173	-1.702	0.091	-11.330	0.856	1858.690	1888.690
	Night Spline Component #1:group	1.226	3.453	244.452	0.355	0.723	-5.575	8.028	1858.690	1888.690
	Night Spline Component #2:group	10.855	5.998	242.572	1.810	0.072	-0.961	22.670	1858.690	1888.690
	Night Spline Component #3:group	0.355	2.771	241.760	0.128	0.898	-5.103	5.813	1858.690	1888.690
SWS (%)	(Intercept)	34.539	11.086	38.574	3.116	0.003	12.108	56.971	1927.799	1957.799
	age	-0.216	0.112	32.155	-1.932	0.062	-0.444	0.012	1927.799	1957.799
	race	1.926	2.423	29.827	0.795	0.433	-3.023	6.876	1927.799	1957.799
	Sex	-0.932	2.436	30.150	-0.383	0.705	-5.905	4.041	1927.799	1957.799
	QIDS	-0.247	0.324	29.819	-0.764	0.451	-0.909	0.414	1927.799	1957.799
	TLFB	-0.054	0.054	29.541	-1.007	0.322	-0.164	0.056	1927.799	1957.799
	Night Spline Component #1	-1.911	5.884	239.757	-0.325	0.746	-13.502	9.679	1927.799	1957.799
	Night Spline Component #2	6.392	10.236	239.882	0.624	0.533	-13.773	26.557	1927.799	1957.799
	Night Spline Component #3	0.339	4.606	239.051	0.074	0.941	-8.734	9.413	1927.799	1957.799
	group	0.528	3.471	117.920	0.152	0.879	-6.345	7.401	1927.799	1957.799
	Night Spline Component #1:group	1.835	3.946	243.606	0.465	0.642	-5.938	9.608	1927.799	1957.799
	Night Spline Component #2:group	-2.959	6.856	241.544	-0.432	0.666	-16.465	10.547	1927.799	1957.799

REM (%)	Night Spline Component #3:group	1.575	3.167	240.690	0.497	0.619	-4.665	7.815	1927.799	1957.799
	(Intercept)	25.276	6.319	59.232	4.000	0.000	12.633	37.920	1819.542	1849.542
	age	-0.061	0.059	36.157	-1.021	0.314	-0.181	0.060	1819.542	1849.542
	race	-1.437	1.250	31.400	-1.150	0.259	-3.984	1.110	1819.542	1849.542
	Sex	1.768	1.262	32.124	1.401	0.171	-0.803	4.338	1819.542	1849.542
	QIDS	-0.374	0.167	31.597	-2.235	0.033	-0.714	-0.033	1819.542	1849.542
	TLFB	-0.004	0.028	31.029	-0.145	0.885	-0.060	0.052	1819.542	1849.542
	Night Spline Component #1	1.783	5.017	250.462	0.355	0.723	-8.099	11.664	1819.542	1849.542
	Night Spline Component #2	9.268	8.725	251.072	1.062	0.289	-7.915	26.451	1819.542	1849.542
	Night Spline Component #3	-0.654	3.928	251.356	-0.167	0.868	-8.390	7.082	1819.542	1849.542
	group	3.107	2.491	215.360	1.247	0.214	-1.803	8.017	1819.542	1849.542
	Night Spline Component #1:group	-0.764	3.344	255.185	-0.229	0.819	-7.349	5.821	1819.542	1849.542
	Night Spline Component #2:group	-4.257	5.828	253.218	-0.730	0.466	-15.734	7.220	1819.542	1849.542
	Night Spline Component #3:group	0.175	2.693	253.809	0.065	0.948	-5.129	5.479	1819.542	1849.542
DSR	(Intercept)	1.305	1.178	31.458	1.108	0.276	-1.096	3.706	777.635	807.635
	age	0.014	0.012	22.487	1.242	0.227	-0.010	0.038	777.635	807.635
	race	-0.145	0.245	19.448	-0.591	0.561	-0.656	0.367	777.635	807.635
	sex	-0.240	0.248	20.284	-0.969	0.344	-0.757	0.277	777.635	807.635
	QIDS	0.004	0.033	19.983	0.121	0.905	-0.065	0.073	777.635	807.635
	TLFB	-0.003	0.005	19.783	-0.552	0.587	-0.014	0.008	777.635	807.635
	Night Spline Component #1	-0.260	0.784	218.533	-0.332	0.740	-1.805	1.284	777.635	807.635
	Night Spline Component #2	-0.517	1.372	216.458	-0.376	0.707	-3.222	2.188	777.635	807.635
	Night Spline Component #3	0.298	0.642	215.622	0.464	0.643	-0.967	1.563	777.635	807.635
	group	0.040	0.416	140.847	0.096	0.924	-0.782	0.862	777.635	807.635
	Night Spline Component #1:group	0.161	0.524	225.110	0.308	0.758	-0.872	1.195	777.635	807.635
	Night Spline Component #2:group	0.592	0.919	217.805	0.644	0.520	-1.219	2.402	777.635	807.635
	Night Spline Component #3:group	-0.115	0.441	217.410	-0.261	0.795	-0.984	0.755	777.635	807.635
REM Density	(Intercept)	9.606	3.283	41.908	2.926	0.006	2.981	16.232	1220.017	1250.017
	age	0.019	0.033	33.290	0.583	0.564	-0.047	0.085	1220.017	1250.017
	race	-0.514	0.693	29.882	-0.742	0.464	-1.928	0.901	1220.017	1250.017
	sex	-1.503	0.711	30.791	-2.115	0.043	-2.953	-0.053	1220.017	1250.017
	QIDS	0.036	0.093	29.899	0.393	0.697	-0.153	0.225	1220.017	1250.017
	TLFB	0.016	0.016	29.955	1.028	0.312	-0.016	0.048	1220.017	1250.017
	Night Spline Component #1	-0.954	1.881	227.778	-0.507	0.612	-4.661	2.752	1220.017	1250.017
	Night Spline Component #2	-6.037	3.413	228.693	-1.769	0.078	-12.762	0.688	1220.017	1250.017
	Night Spline Component #3	-1.845	1.456	226.841	-1.268	0.206	-4.713	1.023	1220.017	1250.017

group	-0.824	1.087	136.720	-0.757	0.450	-2.974	1.327	1220.017	1250.017
Night Spline Component #1:group	0.718	1.252	231.789	0.574	0.567	-1.749	3.186	1220.017	1250.017
Night Spline Component #2:group	2.679	2.214	229.817	1.210	0.227	-1.683	7.041	1220.017	1250.017
Night Spline Component #3:group	0.465	0.979	228.574	0.475	0.635	-1.464	2.393	1220.017	1250.017

Supplementary Files

This is a list of supplementary files associated with this preprint. Click to download.

- Supplement.docx